2016

Zero-Group-Velocity Propagation Of Electromagnetic Wave Through Nanomaterial

Taian Fan
University of Vermont

ZERO-GROUP-VELOCITY PROPAGATION OF ELECTROMAGNETIC WAVE THROUGH NANOMATERIAL

A Thesis Presented

by

Taian Fan

to

The Faculty of the Graduate College

of

The University of Vermont

In Partial Fulfillment of the Requirements
for the Degree of Master of Science
Specializing in Electrical Engineering

May, 2016

Defense Date: March 29th, 2016
Thesis Examination Committee:

Walter Varhue, Ph.D., Advisor
Dryver Huston, Ph.D., Chairperson
Stephen Titcomb, Ph.D.
Tian Xia, Ph.D.
Cynthia J. Forehand, Ph.D., Dean of the Graduate College

ABSTRACT

This research will investigate the problem on the propagation of electromagnetic wave through a specific nanomaterial. The nanomaterial analyzed is a material consisting of a field of Pt nanorods. This field of Pt nanorods are deposited on a substrate which consists of a RuO_2 nano structure. When the nanorod is exposed to an electron beam emitted by a TEM (Transmission electron microscopy). A wave disturbance has been observed. A video taken within the chamber shows a wave with a speed in the scale of um/s ($10^{-6}m/s$), which is 14 orders of magnitude lower than speed of light in free space (approximate $3 \times 10^{8}\mathrm{m/s}$). A physical and mathematical model is developed to explain this phenomenon. Due to the process of fabrication, the geometry of the decorated Pt nanorod field is assumed to be approximately periodic. The nanomaterials possess properties similar to a photonic crystal. Pt, as a noble metal, shows dispersive behaviours that is different from those ones of a perfect or good conductors. A FDTD algorithm is implemented to calculate the band diagram of the nanomaterials. To explore the dispersive properties of the Pt nanorod field, the FDTD algorithm is corrected with a Drude Model. The analysis of the corrected band diagram illustrates that the group velocity of the wave packet propagating through the nanomaterial can be positive, negative or zero. The possible zero-group velocity is therefore used to explain the extremely low velocity of wave (wave envelope) detected in the TEM.

TABLE OF CONTENTS

Page

LIST OF FIGURES

Figure Page

LIST OF TABLES

CHAPTER 1: INTRODUCTION

1.1. Motivation

The propagation of electromagnetic waves through material has one way or another been at the center of a majority of scientific investigation performed throughout the modern science. Maxwell's equations provide a basic theory to help understand this behavior. The rapid development of nanotechnology in recent years has given birth to various kinds of new nanomaterials [1]. Many new experimental and theoretical methods have been invented to study the electromagnetic properties of these nanomaterials [2, 3]. These studies form the basis for a new academic discipline called Nanophotonics or Nano-optics [4]. It focuses on the behavior of electromagnetic radiation on a nanometer scale, and the interaction of nanometer-scale objects with an EM wave. Among all this research, metallic nanomaterials are often involved, and usually the metallic components are used to generate surface plasmon polaritons[5] so that EM waves are transported and focused. As an artificial material, structures of the nanomaterial can be designed. In all possible morphology of the nanomaterial, a particular kind of structure, periodic structures, attracts the greatest attention from scientists and engineers in Nanophotonics. The periodicity of these structures gives the material properties similar to that of a crystal which is formed by periodically located and bonded atoms. Photonic crystal is the name of these materials with a periodic optical nanostructure [6]. On the other hand, metals are dispersive materials. The behavior of a metal at high frequency (ultraviolet or higher) deviates from a good conductor dramatically. Plasmonic devices, with or without periodic structures, explore the possibility of taking advantages of these dispersive

properties of metals. The intersection between these two disciplines, photonic crystal and plasmonic material, can be used to describe periodic metallic nanostructures and to exploit the dispersive properties of metals. Even though these metallic nanostructures are on the order of nanometers, a description and analysis of their behavior can be made without resorting to Quantum Mechanics. The electron energy levels of a metal are still dense enough that the spacings between them are negligible compared to $K_B T$, which is the thermal excitations energy at room temperature, The optics of these metallic nanostructures can still be described using classical Electromagnetic theory[7].

1.2. Material Structure

In this investigation, Pt nanorod decorated/RuO_2 square nanorods have been grown on an aluminized Si substrate surface [8] via a reactive co-sputtering process in an electron cyclotron resonance (ECR) plasma reactor [9].

The TEM pictures of the material are showed in Figure 1 and Figure 2

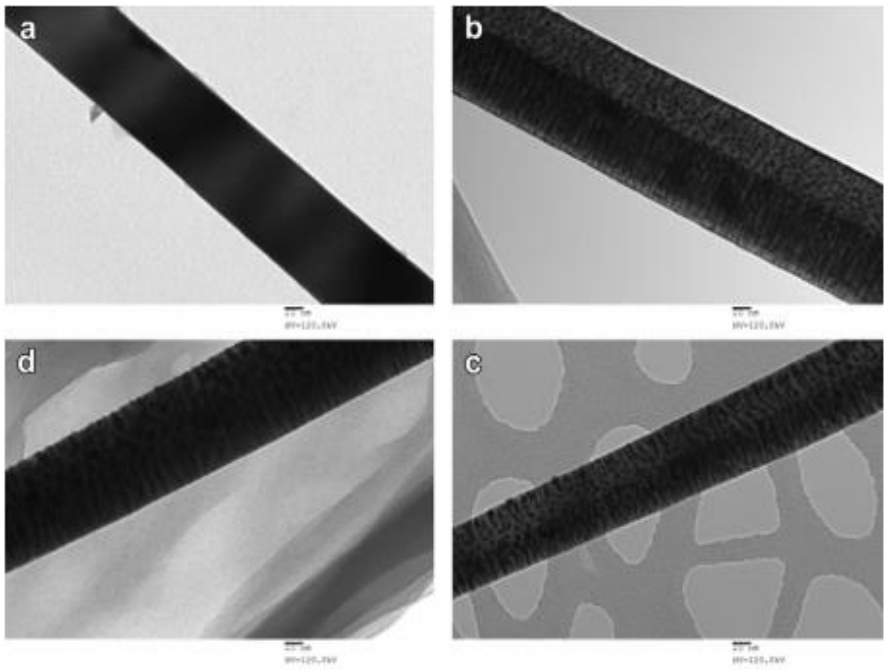

Figure 1:TEM images of RuO2 nanoro detached from the surface. *All films were grown on Al/Si with a total deposition time of 30 min. Shown in (a) are 62 nm wide RuO2 nanorods with no Pt, (b) 84 nm wide RuO2 nanorods with Pt co-sputtered for the last 15 min of the deposition time, (c) 81 nm wide RuO2 nanorods with Pt co-sputtered for the last 20 min of the deposition time, and (d) 89 nm wide RuO2 nanorods with Pt co-sputtered for the last 25 min of the deposition time [8].*

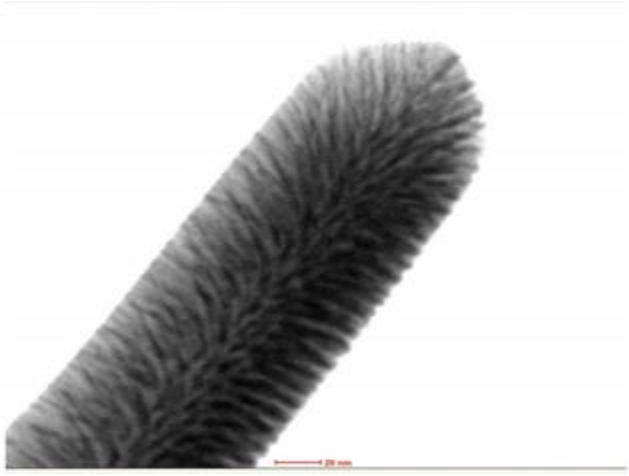

Figure 2:TEM image of an individual nanorod, showing Pt nanorods bending as the bulk RuO2 nanorods continues to grow. The Pt was co-sputtered for the final 20 min of the 30 min of total deposition [8].

To further analyze the material, a geometrical model is required to represent the material, to further assisting the analysis with mathematical model, especially reducing the computational resources to make the simulations and analysis acceptable, simplification for the geometrical model is required. Here are three sets of representations and simplifications of the morphology of the nanomaterial.

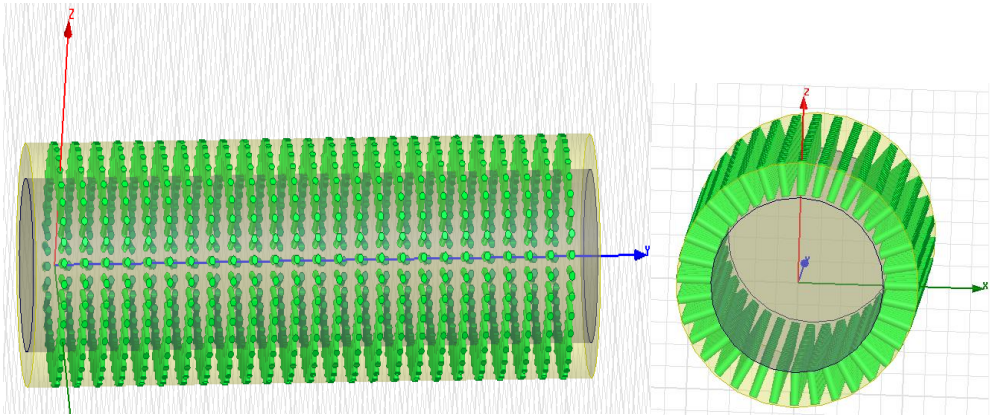

(a) (b)

Figure 3: Pt nanorods (smaller ones on the surface) surrounded by RuO2 (above the surface and around the Pt nanorods) on the surface of an aluminized Si substrate in different views (a) and (b)

In Y direction, the model is periodic, while in X or Z directions, it is not periodic, it is only rotationally symmetrical. Mathematically, it requires a complete 3D model to be built to perform the simulation (using FDTD algorithm in this investigation). That would require a substantial amount of computational resources. So even though this model is the most accurate, simplifications are required.

In XOZ plane, the pt nanorods forms a circle and they are not parallel to each other. However, if we assume Pt nanorods are close enough, and considering their dimension is much smaller compared to that of the substrate, then in a limited area, the Pt nanorods can be assumed to be parallel to each other. A vivid analogy is that people stand on the earth surface which could be treated as flat in a limited area and people are "parallel" to each other. In reality, since the aluminized substrate is cuboid before co-sputtering [18]. The cross section of the substrate after sputtering is more likely to be bouffant rectangular. This makes the assumption that the Pt nanorods are parallel more realistic.

Under the assumption that the Pt nanorods are parallel, the model can be simplified to a 3D model that is periodic in 2 dimension (x and y). In other words, it is two dimensional periodic structure. Figure 4 shows the 2D periodic model in 3D view and from above

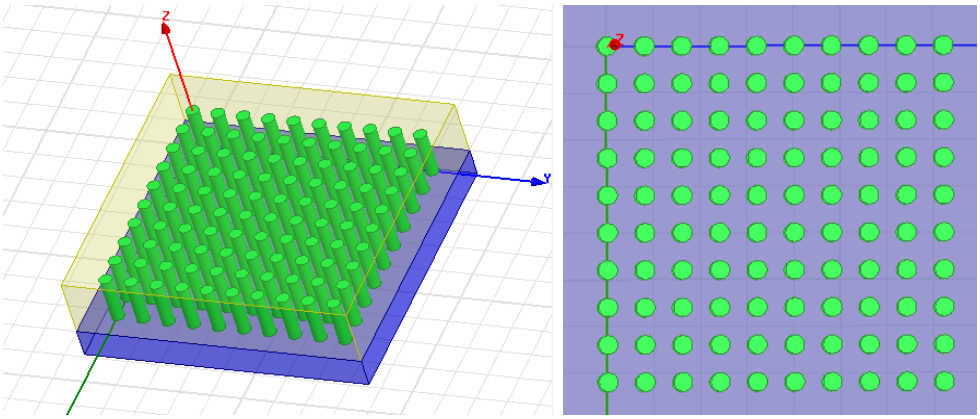

(a) (b)

Figure 4:(a)2D periodic structure, periodicity along both X and Y directions. (b) top view of 2D periodic structure

Since in XOZ plane the Pt nanorods are only rotationally symmetrical. If we assume the adjacent nanorods in x directions are completely isolated from each other, then the nanorods are only periodic along Y directions. However, this assumption will make this model the least accurate, since even though the adjacent nanorods are not periodic in x direction, they still interact with each other strongly due to the small spacing between them.

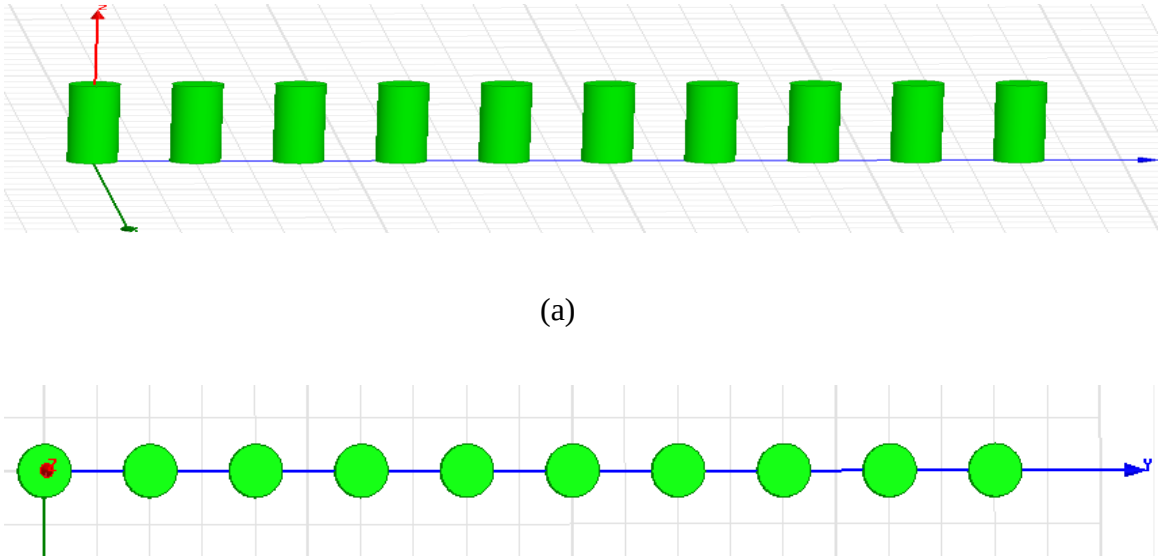

(a)

(b)

Figure 5: (a) 1D periodic structure, periodicity only in the Y direction. (b) Top view of the structure

The second model in figure 4 and third model in figure 5 can both be simulated by implementing a 2D model instead of a 3D one. It will reduce the computational resource required to perform the analysis dramatically.

1.3 Process of Videos

This investigation originated from two videos taken within the chamber of a TEM. Several different frames extracted from videos (original color and fake color) are presented for comparison. Since in black and white pictures the wave is weak compared to the background, fake color was implemented to enhance these frames.

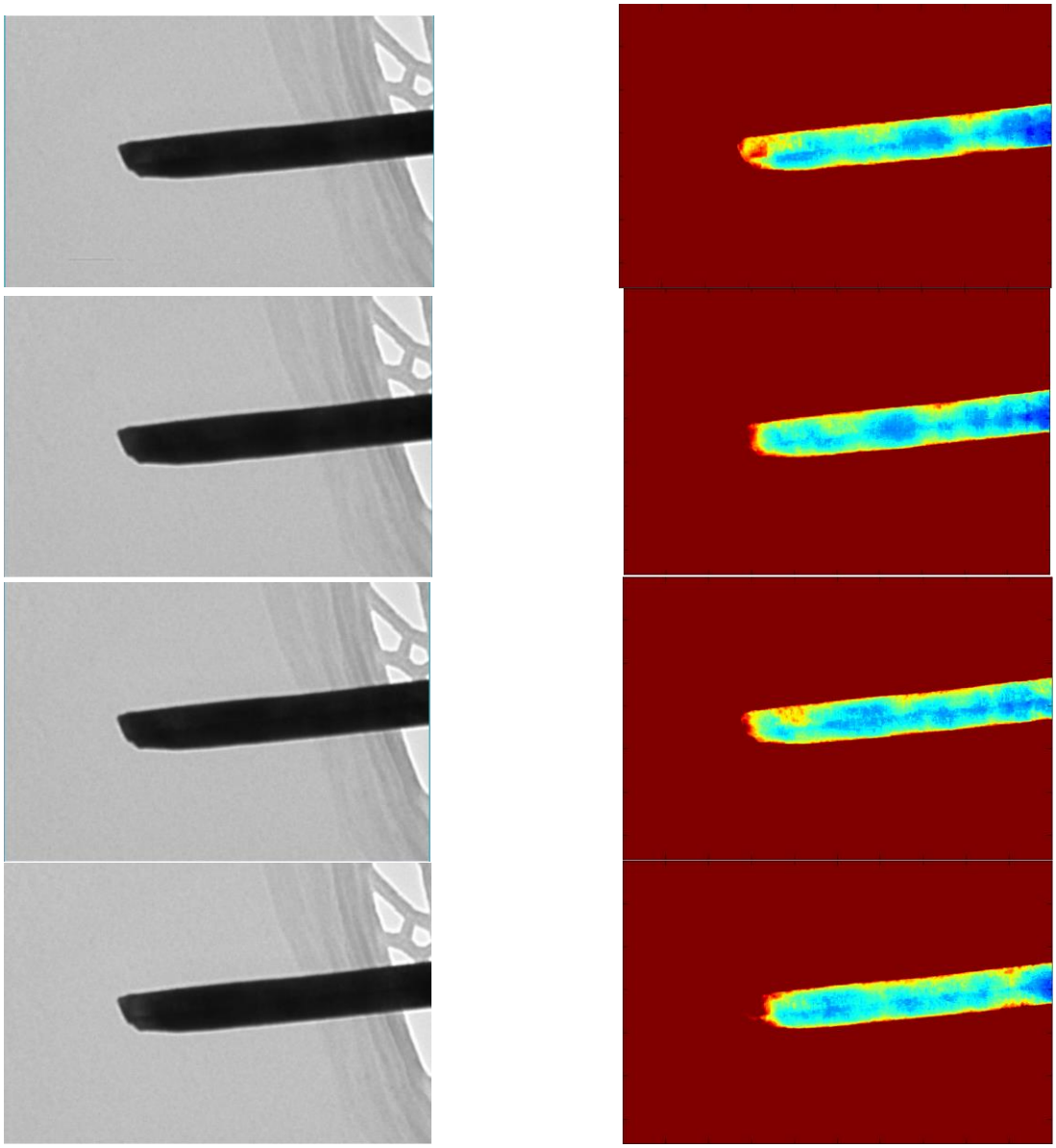

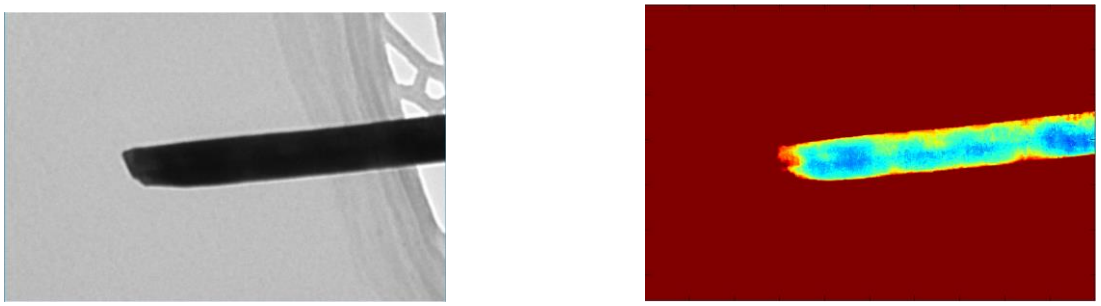

(a) (b)

Figure 6: Frames extracted from first video in original color (a) corresponding frames after fake color enhancement (b)

Figure 6 are the frames from the fist video used in the velocity calculation, two frames from another video and the corresponding fake-color frames are showed as follow:

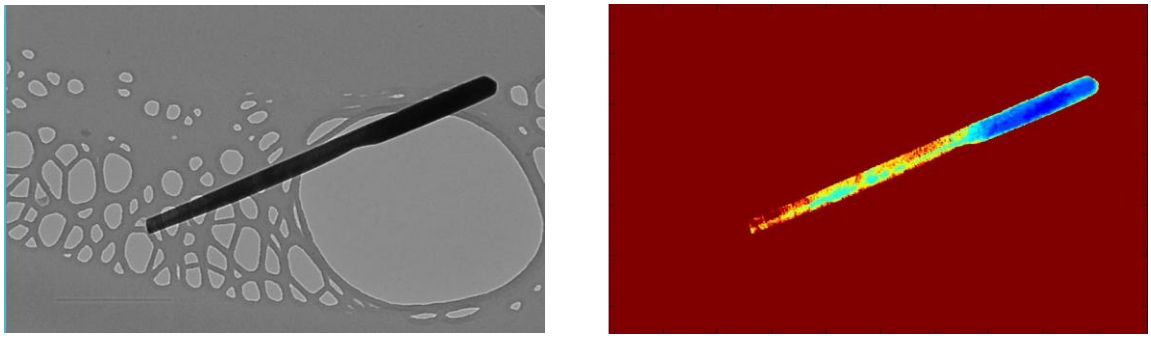

(a) (b)

Figure 7: Frames extracted from second video in original color (a) frames after fake color enhancement (b)

The analysis of the wave front frame by frame suggests that the velocity of the wave is 0.75um/s or $0.75 \times 10^{-6} m/s$, which is a very small number. Here is a comparison of this velocity with some common velocities in Electromagnetism and solid

physics: The speed of light is in the order of $10^8 \mathrm{m/s}$, the thermal velocity of the electrons is in the order of $10^5 m/s$. One of them is 100 trillion times (14 orders of magnitude) faster, the other is 100 billion times (11 orders of magnitude) faster.

The velocity of the wave is so low. In all theories and concepts related to velocity of waves, group velocity provides a possible explanation to this extremely low velocity. In next chapter, the theories and concepts related to group velocity are briefly reviewed.

CHAPTER 2: PHASE VELOCITY AND GROUP VELOCITY

2.1. Phase Velocity

Phase velocity and group velocity are closely related, usually they are explained together. Before explain them, some fundamental concepts of wave propagation should be reviewed in advance.

For a pure sinusoidal monochromatic wave that travels in the positive x direction, its mathematical representation is as follow:

$$s(x,t) = A\cos(\omega t - kx)$$

Where $\omega = 2\pi/T = 2\pi f$ is the angular frequency, $k = 2\pi/\lambda$ is the wave number, λ and f are the wavelength and frequency.

The phase velocity of a wave is the velocity with which phase fronts propagate in a medium. It is related to the wavenumber and the angular frequency as follow:

$$v_{ph} = \frac{\omega}{k}$$

The phase velocity is defined as giving the phase difference between the vibrations observed at two different points in a free plane [10].

2.2. Group Velocity

General formulation of group velocity can be found in [11, 12]. For ease of reference, we quote the major results in this section.

Group velocity is the velocity of wave envelop or modulation of the wave that propagates through space. Consider two sinusoidal signals: $A_0\cos(\omega_1 t - k_1 x)$ and $A_0 \cos(\omega_2 t - k_2 x)$, the angular frequencies ω_1 and ω_2 are slightly different.

$$S(x,t) = A_0\cos(\omega_1 t - k_1 x) + A_0 \cos(\omega_2 t - k_2 x)$$

$$= 2A_0 \cos\left(\frac{\omega_1-\omega_2}{2}t - \frac{k_1-k_2}{2}x\right)\cos\left(\frac{\omega_1+\omega_2}{2}t - \frac{k_1+k_2}{2}x\right)$$

Since ω_1 and ω_2 are only slightly different, so $\frac{\omega_1+\omega_2}{2}$ is close to ω_1 or ω_2, while $\frac{\omega_1-\omega_2}{2}$ is a small number which represents a much lower frequency, so that $\cos\left(\frac{\omega_1-\omega_2}{2}t - \frac{k_1-k_2}{2}x\right)$ modulates the amplitude of the overall signal.

$$\Delta\omega = \omega_1 - \omega_2$$

$$\Delta k = k_1 - k_2$$

The velocity of the modulation is $\frac{\Delta\omega}{\Delta k}$, consider the limit $\Delta k \to 0$

$$v_{gr} = \partial\omega/\partial k$$

This eqution defines the group velocity .

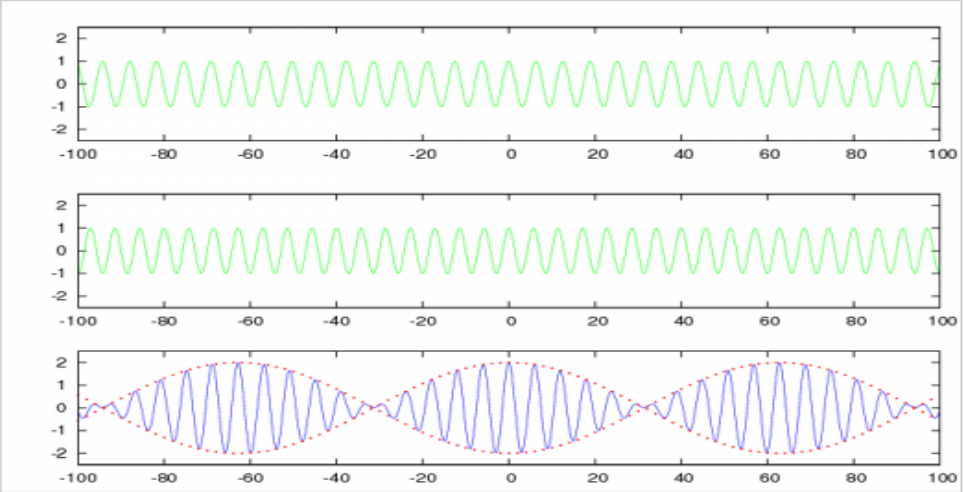

Figure 8:The signals of first and second row plots, with slightly different frequencies are added generating the bottom plot signal [11]

2.3. Dispersion Relationship

In optics, dispersion is the phenomenon by which the group velocity of light in transparent medium is related to the optical frequency or wavelength [12].

Dispersion relations are most commonly expressed in terms of angular frequency $\omega = 2\pi f$ and wavenumber $k = 2\pi/\lambda$。

$$\omega(k) = v(k) \cdot k$$

As showed in figure 9, on the dispersion curve, the phase velocity v_{ph}at point P is the slope of the line connecting point P and the origin O. The group velocity v_{gr} at point P is the slope of the tangent line that runs through point P.

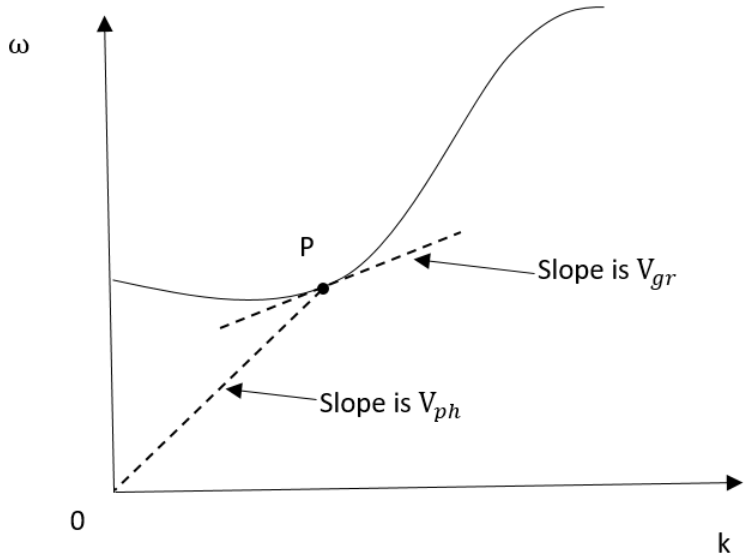

Figure 9: Dispersion relationship, phase velocity and group velocity

CHAPTER 3: PHOTONIC CRYSTAL

3.1. Introduction to Photonic Crystal

Photonic crystals are electromagnetic media with periodic structures. This periodicity in structure is analogous to a crystal lattice. The wave function of the electron is modulated by the atomic lattice resulting in a band of allowed and forbidden energy levels. The phenomenon of electron energies in a crystal are routinely studied in solid state physics and the results are widely applied to the semiconductor industry [14]. The analysis of bandgap in the solid physics is achieved generally by applying the Bloch's description of periodic potential to the solution of Schrodinger's equation [13]. It is Schrodinger' equation that governs the behavior of electrons. By analogy, the Bloch's theorem can also be applied to describe the periodically structured photonic crystals, and Maxwell's equations, which describe the behavior of photons, are mathematically similar to the Schrodinger's equation. Hence the bandgap of the photons in photonic crystal is predicted by the theory and can be observed in the lab [6].

The propagation of electromagnetic wave through periodic structure was first studied by Lord Rayleigh in 1887[15]. His study focused on the one-dimensional photonic crystal, which is a periodic multi-layer thin films with different dielectric constants. He pointed out that for a certain range of frequency, the light propagation is prohibited. This forbidden band corresponds to a bandgap. A bragg reflector is a classical one-dimensional photonic crystal. It produces different colors which vary with the angle of incidence. A similar phenomena can be observed on certain butterfly wings.

Intensive research has been conducted on one-dimensional periodic thin films in the last century. Many products have resulted from the application of this technology.

In 1987, Yablonovitch[16] and John[17] extended the periodicity from one dimension to two dimension and three dimension. Their principles, combined the analytical tools in electromagnetism and solid physics, finally giving the devices the name photonic crystal. After 1987, the research related to photonic crystals has advanced dramatically, not only confined to theory, but also in fabrication and methods of analysis, especially numerical ones.

3.2. Maxwell's Equations in Periodic Media

The propagation of wave through three-dimensionally periodic media was studied by Felix Bloch in 1828. His theory unknowingly advanced the study of Gaston Floquet in 1883[18, 19] from one-dimension to three-dimension. According to Bloch's research, waves can propagate through periodic structure without scattering, the overall wave can be expressed as a periodic envelope function multiplied by a plane wave. Bloch proved this theory in the context of quantum mechanics governed by Schrodinger's equation. Due to similarities between Schrodinger's equation and Maxwell's equations. A theory for wave propagation in periodic media can be given. This technique is further applied to Maxwell's equations [6].

Assume there is no free electric or magnetic charges in the material, also assume the field is time dependent $e^{-i\omega t}$, and $\mu_r \equiv 1$, hence the Faraday's and Ampere's equations are，

$$\nabla \times \vec{E} = -\mu_0 \frac{\partial \vec{H}}{\partial t} = -i\omega\mu_0 \vec{H}$$

$$\nabla \times \vec{H} = \varepsilon_0 \varepsilon_r \frac{\partial \vec{E}}{\partial t} = i\omega\varepsilon_0 \varepsilon_r \vec{E}$$

Applying curl to the second equation yields:

$$\nabla \times \left(\frac{1}{\varepsilon_r} \nabla \times \vec{H}\right) = i\omega\varepsilon_0 \left(\nabla \times \vec{E}\right) = -\varepsilon_0\mu_0 (i\omega)^2 \vec{H} = \varepsilon_0\mu_0\omega^2 \vec{H} = (\frac{\omega}{c})^2 \vec{H}$$

$$\nabla \times \left(\frac{1}{\varepsilon_r} \nabla \times \vec{H}\right) = (\frac{\omega}{c})^2 \vec{H}$$

This is the master equation.

$\nabla \times \frac{1}{\varepsilon_r} \nabla \times \vec{H}$ is an Eigen-operator [16], $\vec{H}$ is the Eigen-state, $(\frac{\omega}{c})^2$ is the eigen-value. For real (lossless) ε_r , the Eigen-operator is Hermitian. The solution of the equation is now an Eigen-value problem, and via linear algebra, there are several properties: ω is real (lossless), Eigen-states are orthogonal, Eigen-states are complete [6, 20].According to the the Bloch-Floquet theorem, if the Eigen-operator is periodic, the solution takes the form:

$$\vec{H}(\vec{x}, t) = e^{i(\vec{k}\cdot\vec{x} - \omega t)} \vec{H}_{\vec{k}}(\vec{x})$$

$e^{i(\vec{k}\cdot\vec{x}-\omega t)}$ is the classic expression for a plane wave, and the $\vec{H}_{\vec{k}}(\vec{x})$ is the envelop that is periodic. Its periodicity is defined in the reciprocal vector space, which is mapped from the primitive vector space [6, 13]. To further explain the reciprocal vector that is used to describe the periodicity of the solutions and the relationship between reciprocal vector space and primitive vector space, a brief review of the concepts related to periodic structures is presented below.

3.3 Mathematical Descriptions of Periodic Structures

Periodic structures are most widely studied in solid state physics and crystallography to describe the structure of crystals. Many of the basic mathematical definitions and tools possess names associated with crystal, but the theories and techniques can be applied to periodic structures in a photonic crystal. The general formulation of periodic structures can be found in [13, 21, 38]. For ease of reference, the major results are conveyed in section 3.3.1, 3.3.2, 3.3.3.

3.3.1. Classification of periodic structures

There are an infinite number of ways that structures can be periodic. We classify periodic structures into: 230 space groups, 32 point groups, 14 Bravais lattices, 7 crystal systems. These classifications are done by apply different, but closely related mathematical criteria like symmetry, rotational invariance, fixation of origin and so on. Among these two concepts are of most concern in this investigation**.**

Bravais Lattices

– Set of all possible ways a lattice can be periodic if composed of identical spheres placed at the lattice points. – 14 Bravais lattices

Crystal Systems

– Set of all Bravais lattices that have the same holohedry (shape of the conventional unit cell) – 7 crystal systems

Table 1: The relationship between three-dimensional crystal families, crystal systems, and lattice systems is shown in the following table [21]:

Crystal family	**Crystal system**	**Required symmetries of point group**	**Point groups**	**Space groups**	**Bravais lattices**	**Lattice system**
Triclinic		None	2	2	1	Triclinic
Monoclinic		1 twofold axis of rotation or 1 mirror plane	3	13	2	Monoclinic
Orthorhombic		3 twofold axes of rotation or 1 twofold axis of rotation and two mirror planes.	3	59	4	Orthorhombic
Tetragonal		1 fourfold axis of rotation	7	68	2	Tetragonal
Hexagonal	Trigonal	1 threefold axis of rotation	5	7	1	Rhombohedral
				18	1	Hexagonal
	Hexagonal	1 sixfold axis of rotation	7	27		
Cubic		4 threefold axes of rotation	5	36	3	Cubic
Total: 6	7		32	230	14	7

Bravais lattice in two dimensions are showed as follow:

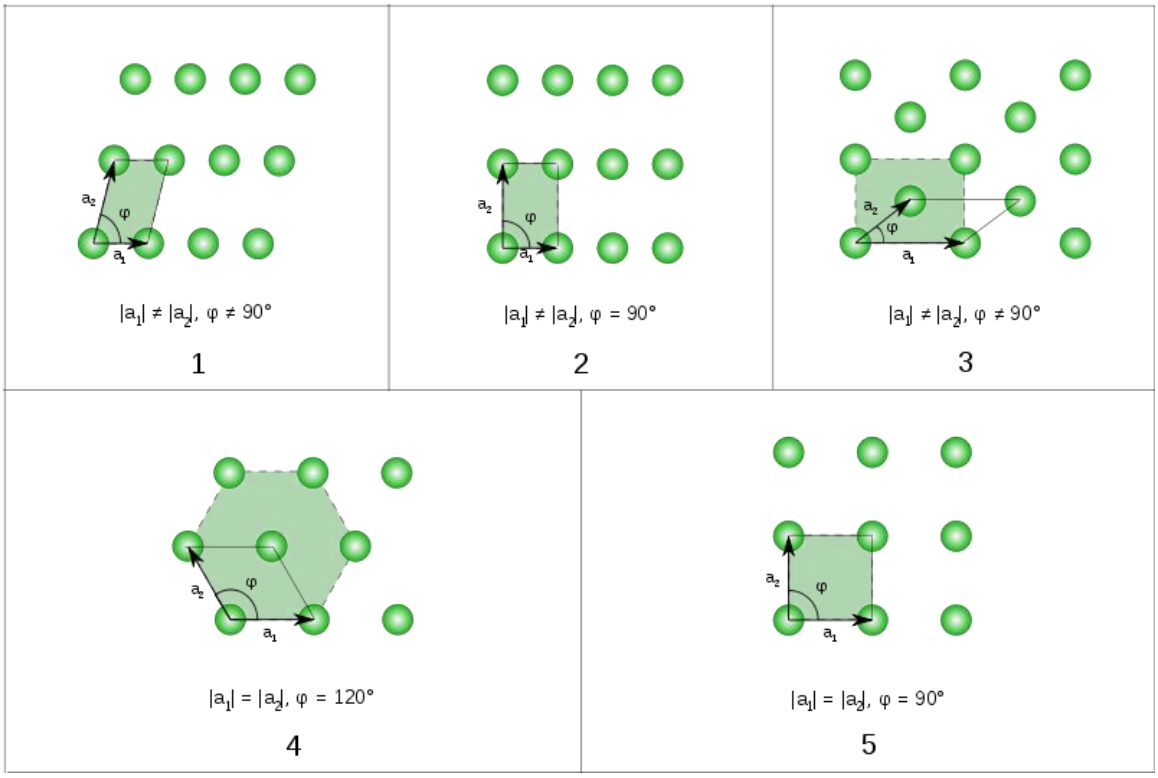

Figure 10: The five fundamental two-dimensional Bravais lattices: 1 – oblique, 2 – rectangular, 3 – centered rectangular, 4 – hexagonal (rhombic), and 5 – square [22].

3.3.2. Primitive Lattice Vector and Reciprocal Lattice Vector

The lattice in three dimensions can be defined by three translation vectors: $\vec{t}_1$, $\vec{t}_2$, $\vec{t}_3$, such that the arrangement of the atoms in the crystal looks the same when viewed from point $\vec{r}$ translated by an integral multiple of the $\vec{t}'s$ [13].

$$\vec{t}_{pqr} = p\vec{t}_1 + q\vec{t}_2 + r\vec{t}_3$$

Here p, q and r are arbitrary integrals.

Translation vectors connect adjacent points in the lattice and can uniquely describe all 14 Bravais lattices. Primitive translation vectors are the smallest possible translation vectors that still describe the unit cell.

The primitive translation vectors are often chosen as primitive axis vectors (not always), the Primitive Lattice vector are also referred as primitive translation vectors. Since the primitive lattice vector describes the lattice existing in the real space, so the lattice it describes is also called a direct lattice, the volume of the primitive lattice cell is $\mathrm{V} = |\vec{t}_1 \cdot \vec{t}_2 \times \vec{t}_3|$.

Every direct lattice is associated with a unique reciprocal lattice, they are connected to each other by a Fourier Transformation. The direct lattice describes the periodic structure. The reciprocal lattice determines how the periodic structure interacts with waves.

Reciprocal lattice vectors,$\vec{K}$, are defined by the following condition:

$$e^{i\vec{K}\vec{R}} = 1$$

Where $\vec{R}$ is a real space lattice vector. Any real lattice vector may be expressed in terms of the lattice basis vectors, $\vec{t}_1, \vec{t}_2, \vec{t}_3$.

$$\vec{R} = c_1\vec{t}_1 + c_2\vec{t}_2 + c_3\vec{t}_3$$

in which the , c_1, c_2, c_3 are integers. The condition on the reciprocal lattice

vectors may also be expressed as

$$\vec{K} \cdot \vec{R} = 2\pi n$$

Where n is an integer. This expression can be satisfied if $\vec{K}$ is expressed in terms of the reciprocal lattice basis vectors $\vec{b}_i$, which are defined as

$$\vec{b}_1 = \frac{2\pi \vec{t}_2 \times \vec{t}_3}{\vec{t}_1 \cdot \vec{t}_2 \times \vec{t}_3}$$

$$\vec{b}_2 = \frac{2\pi \vec{t}_3 \times \vec{t}_1}{\vec{t}_1 \cdot \vec{t}_2 \times \vec{t}_3}$$

$$\vec{b}_3 = \frac{2\pi \vec{t}_1 \times \vec{t}_2}{\vec{t}_1 \cdot \vec{t}_2 \times \vec{t}_3}$$

Note that $\vec{b}_2$ and $\vec{b}_3$ are given by cyclic permutations of the expression for $\vec{b}_3$. From this expression it may be seen that the real lattice basis vectors and the reciprocal lattice basis vectors satisfy the following relation:

$$\vec{b}_i \cdot \vec{t}_j = 2\pi \delta_{ij}$$

Where δ_{ij} is the Kronecker delta, which takes the value 1 when *i* is equal to *j*, and 0 otherwise. Any reciprocal lattice vector may then be expressed as a linear sum of these reciprocal basis vectors:

$$\vec{K} = h\vec{b}_1 + k\vec{b}_2 + l\vec{b}_3$$

In which h, k and l are integers. The set of all $\vec{K}$vectors defines the reciprocal lattice. The space the reciprocal lattice exists is called reciprocal space. Besides, the

corresponding primitive lattice and reciprocal lattice are naturally Fourier Transformation of each other [13].

The properties of $\vec{K}$ can be summarized as follow:

$\vec{K}$ has a unit of 1/length. Similar to the wave-vector k in the plane wave expression e^{ikr}

$\vec{K}$ has a meaning in Fourier transform, k-space, or momentum space.

It defines a set of lattice points in the k-space.

3.3.3. Brillouin Zone and Irreducible Brillouin Zone (IBZ)

The Brillouin zone is a Wigner-Seitz cell of the reciprocal lattice, which is the Fourier transform of the Bravais lattice and the construction of a Brillouin Zone of a 2D square lattice, and can be found at [31].

The first Brillouin Zone after construction is showed as below

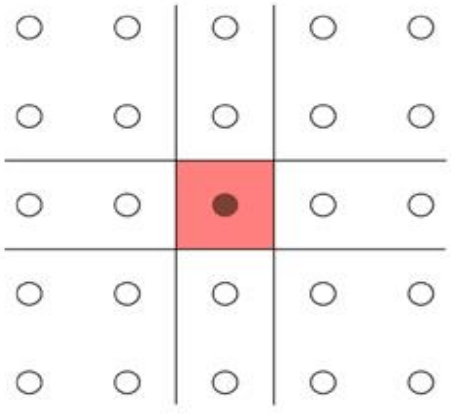

Figure 11: First Brillouin Zone

The smallest region within the Brillouin zone are not related by symmetry (rotations, reflections, and inversions) is called the irreducible Brillouin zone (IBZ). Knowing the solution inside the IBZ is equivalent to knowing the all solutions inside the Reciprocal lattice, (By applying rotation and reflections and inversions).

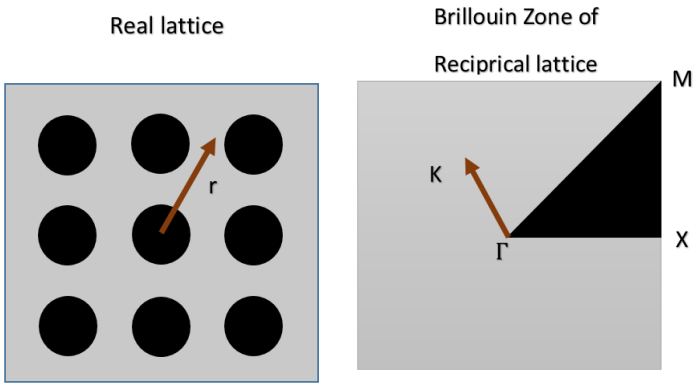

Figure 12: A Square Real lattice, the corresponding Brillouin Zone and Irreducible Brillouin Zone (IBZ).

3.3.5. Bloch-Floquet Theorem

The field inside a periodic structure takes on the same symmetry and periodicity of that structure. It is called Bloch-Floquent Theorem.The mode of a three-dimensional periodic system are Bloch states that can be labelled by a Bloch wave vector $\vec{K} = h\vec{b}_1 + k\vec{b}_2 + l\vec{b}_3$ where $\vec{K}$ lies in the Brillouin zone.

$$\vec{H}_k(\vec{r}) = e^{i\vec{K}\vec{r}}u_k(\vec{r})$$

Where $u_k(\vec{r})$ is a periodic function on the lattice: $u_k(\vec{r}) = u_k(\vec{r} + \vec{R})$ from all lattice vector $\vec{R} = a\vec{t}_1 + b\vec{t}_2 + c\vec{t}_3$ in primitive lattice vectors. The Bloch wave vector $\vec{K}$ here is indeed the reciprocal lattice in the reciprocal space mapped from the primitive lattice defined by the direct lattice vector basis $\vec{t}_1, \vec{t}_2, \vec{t}_3$.

CHAPTER 4: DRUDE MODEL ASSISTED FDTD ALGORITHM IN CALCULATION OF BAND DIAGRAM

4.1 Brief introduction to FDTD algorithm

Many numerical methods have been invented to simulate the electromagnetic environment, such as FDTD, FEM, PWE and so on [41,42]. In this investigation, FDTD is chosen to be implemented to solve the band diagram (i.e. dispersion relations) of our periodic nano structure.

FDTD (Finite-difference time-domain), also known as Yee's method is a numerical analysis technique proposed by Kane S. Yee in 1966 for modelling computational electromagnetics[23]. The FDTD applied discretization to Maxwell's equations in Partial differential form. More specifically, the space and time partial derivatives in Maxwell's equations are discretized by central-difference approximations. The FDTD method is arguably the simplest, both conceptually and in terms of implementation, of the full-wave techniques used to solve problems in electromagnetics [24]. This simplicity broadens the applications of this technique dramatically, while making the computation more complicated and requiring a heavy amount of computational resources when solving complex problems.

Figure 13 shows the spatial arrangement of the Electric and magnetic fields:

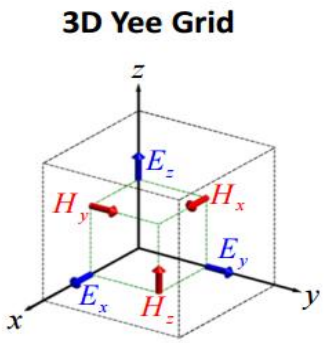

Figure 13: 3D Yee's grid

In time domain gap equal to half of is set between the time step electric fields and the magnetic fields. In other words, arrange $\overrightarrow{E}$ ($\overrightarrow{D}$) and $\overrightarrow{\mathrm{H}}$ in different time so that $\overrightarrow{E}$ ($\overrightarrow{D}$) exists at integer time steps (0, Δt, 2Δt,⋯) while $\vec{H}$ exists at half time steps (Δt/2, t+Δt/2, 2t+Δt/2,⋯). After the discretization in both temporal and spatial domain. An updating loop can be formed to simulate the Electromagnetic environment. Figure 14 shows general H-E updating sequence. The underlying assumption is that the material is linear, isotopic and non-dispersive.

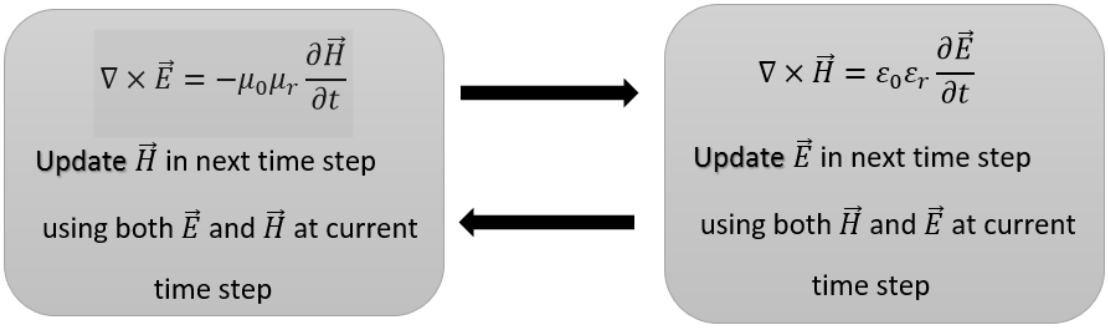

Figure 14: H-E updating sequence

4.2 Brief Introduction to Drude Model

Over all the frequency dependent model used to describe the optical properties of metal. The Drude model, or a plasma model is one of the most widely used models. It was proposed by Paul Drude in 1900 [34, 35]. Its underlying assumption is that the positive charge ions inside the material (especially metals) can be treated immobile while a 'sea' of restless electrons were detached from these heavier cores. This assumption is the natural result of applying kinetic theory on electrons and ion cores. In Drude model interactions between electrons or between electrons and ions are simplified so that any long range effect was neglected. Instantaneous collision between electrons and the ions cores and the Coulomb force between them [36]. The Drude model can be furtherly extended as Drude–Lorentz model and Drude–Sommerfeld model. The classic form of Drude model for dielectric constant are expressed as follow:

$$\tilde{\varepsilon}_r(\omega) = 1 - \frac{\omega_p^2}{\omega^2 - j\omega\Gamma}$$

$$\omega_p = \frac{Nq^2}{\varepsilon_0 m_e}$$

$$\tau = \frac{1}{\Gamma}$$

ω_p is the plasma frequency, q is the electric charge of electron, m_e is the effective mass of the electron, N is the number of electrons per unit volume, τ is mean collision rate or the momentum scattering time

Note that the Drude model itself already considers the effect of the conductivity

$$\tilde{\varepsilon} = \varepsilon_0 \tilde{\varepsilon}_r = \varepsilon_0 \left(1 - \frac{\omega_p^2}{\omega^2 - j\omega\Gamma}\right) = \varepsilon(\omega) - \frac{\sigma(\omega)}{i\omega}$$

$$\varepsilon(\omega) \equiv \varepsilon_0$$

$$\sigma(\omega) = \frac{i\omega\varepsilon_0\omega_p^2}{\omega^2 - i\omega\Gamma}$$

Besides, $\tilde{\varepsilon}_r(\omega) = 1 + \chi(\omega)$

So the susceptibility is given by

$$\chi(\omega) = -\frac{\omega_p^2}{\omega^2 - j\omega\Gamma}$$

With the Drude model, Pt can be simulated as a dispersive material, which is more realistic at optical frequencies [7].

4.3 FDTD Algorithm Incorporating Drude Model

The H-E updating sequence cannot be used any more since its underlying assumption is compromised by the Drude model. Instead an H-D-E method is implemented. In this method the constitutive relationship between D and E is isolated from the Ampere's law and the Drude model is then incorporated into the relationship.

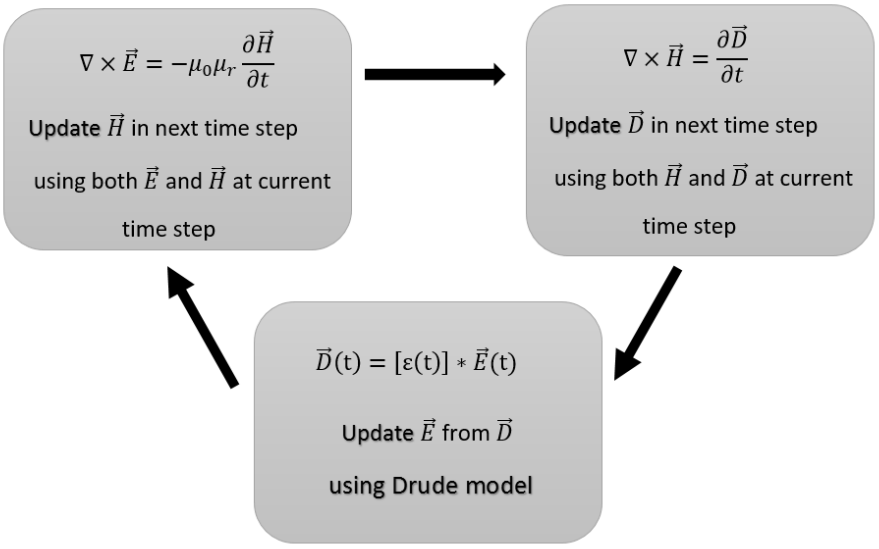

Figure 15: H-D-E updating sequence

The numerical formulation of Constitutive relationship used in this investigation are showed in Appendix A.

4.4 Other Auxiliary Algorithms Incorporated in FDTD

4.4.1 Brief Introduction to Perfect Matched Layer

A perfect matched layer (PML) is an artificial layer that locates at the boundary of the simulation area. It is used to absorb the outgoing waves. Theoretically, for an open boundary system the electromagnetic waves can propagate to infinity, the simulation area will increase dramatically to infinity at last if every point the wave front go through is simulated. However, the computational resource is always limited. The PML is invented to tackle this conflict. The incident waves from all angles will be absorbed by the PML so that no reflection exists at the surface of the PML. Hence the wave propagated on the PML

can still be regarded as outgoing while the simulation area is confined within the external boundary of PML. Figure 16 below is a presentation of a 2D PML.

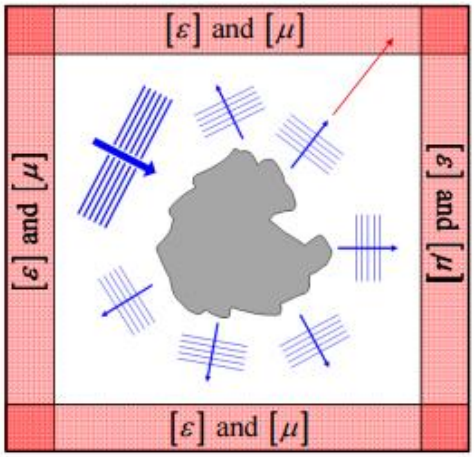

Figure 16: Uniaxial perfect matched layer [25]

PML is first introduced by Berenger[27], after that several equivalent realizations of PML have been developed. The original Berenger's realization is classified as split-filed PML, since in his work every field component is split into two new artificial parts. Other than splitting field, coordinate stretching [28, 29] are most widely used. Besides, several specialized PML realizations truncated for advanced individual FDTD algorithms have also been developed [30, 31]. In this research, I implement Uniaxial PML (UPML) for its straightforwardness and efficiency. It can be treated as a special case of more generalized complex coordinate stretching method [32]. UPML can be derived by analysing scenario of incident wave with arbitrary angles and polarization and then solving the conditions in which there is no reflections. An artificial anisotropic absorbing layer is constructed at the

boundary of the simulation area [33]. PML will be used in the simulation of 1D periodic structure in this investigation [25, 39].

4.4.2 Bloch Periodic Boundary Conditions

Recall Chapter 3, according to Bloch theorem, the field inside a periodic structure should satisfy:

$$\vec{A}_k(\vec{r}) = e^{i\vec{K}\vec{r}}u_k(\vec{r})$$

Where $u_k(\vec{r})$ is a periodic function on the lattice: $u_k(\vec{r}) = u_k(\vec{r} + \vec{R})$ from all lattice vector $\vec{R} = a\vec{t}_1 + b\vec{t}_2 + c\vec{t}_3$ in primitive lattice vectors. The Bloch wave vector $\vec{K}$ here is indeed the reciprocal lattice in the reciprocal space mapped from the primitive lattice defined by the direct lattice vector basis $\vec{t}_1, \vec{t}_2, \vec{t}_3$.

Then
$$\vec{A}_k(\vec{r} + \vec{R}) = e^{i\vec{K}(\vec{r}+\vec{R})}u_k(\vec{r} + \vec{R})$$

$$= \left[e^{i\vec{K}\vec{r}}u_k(\vec{r})\right]e^{i\vec{K}\vec{R}}$$

$$= \vec{A}_k(\vec{r})e^{i\vec{K}\vec{R}}$$

If we set $\vec{R} = \vec{t}_1 + \vec{t}_2 + \vec{t}_3$ as lattice vector for primitive unit cell. Then any field at the boundary of the unit cell can be expressed as the field across the unite cell multiplied by a plane wave with Bloch wave vector as its wave number. This is the exact Bloch periodic Boundary conditions. The detailed implementation of periodic boundary condition can be found [25, 39].

4.5 General Procedure of Band Diagram Calculation

The detailed procedure of band diagram calculation can be found at [25, 40]. Here is a summary of the general procedure:

1 create the primitive lattice (primitive unit cell) with or without PML boundary.

2 apply periodic boundary conditions to the primitive lattice with specific Bloch wave vector.

3 generate multiple dipole sources in the primitive lattice. The locations of the dipole sources are randomly chosen, they should not be obviously symmetric. The polarization of the dipole sources should also be random. These setup is implemented to excite all the possible modes.

4 choose multiple randomly distributed points to record the field components throughout the simulation time.

5 Fourier transform (FFT) the recorded fields to calculate the poser spectral density (PSD) respectively, then sum up the all the results.

$$\mathrm{PS}D_p(\omega) = \left| FFT\{E_z^p(t)\} \right|^2$$

$$\mathrm{PSD}(\omega) = \sum_p \mathrm{PS}D_p(\omega)$$

6 the eigen-frequencies of the Bloch modes are identified as sharp peaks in overall PSD,

7 Repeat step 2 to step 6 for all the Bloch vectors interested.

8 plot the eigen-frequencies as a function of the Bloch wave vectors.

As for the choice of the Bloch vectors, vectors along the edge of the Irreducible Brillouin Zone are the set of vectors mostly commonly used.

In this chapter, only general introduciton to the algorithm is made, the implementation of the algorithm require more details, espeically the structure of the algorithm and the detailed update equations. In this investigation, knowledge from references [24,25,26] are most heavily used, please refer to these references for more comprehensive and detailed information.

CHAPTER 5: RESULTS AND DISCUSSION

5.1 2D Band Diagram (Dispersion Relations)

Here is the 2D periodic model being simulated. It has been showed in Chapter 1, we copied it here to assist the understanding the procedure of calculating direct lattice, reciprocal lattice and Bloch Wave vector.

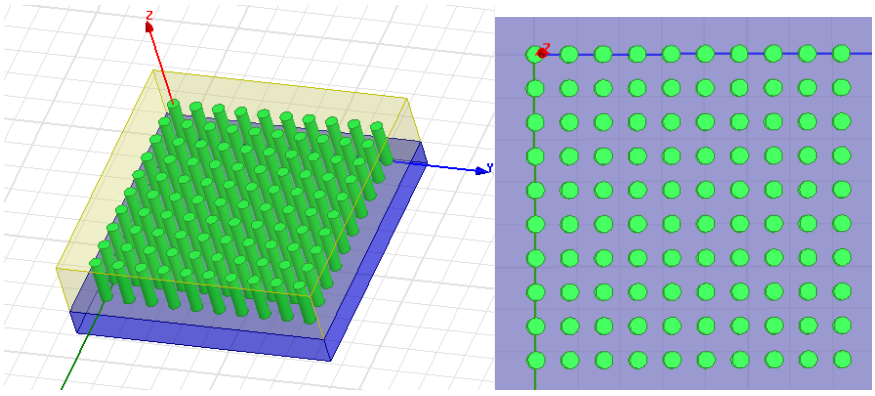

(a) **(b)**

(a) 2D periodic model in 3D view, periodic in both x and y directions and infinitely long in z direction (b) plane 2D view, from above

The choice of direct lattice, calculation of reciprocal lattice and irreducible Brillouin zone (IBZ) are showed in figure 17, and in Figure 18, the choice of the Bloch wave vector was presented, they are chosen along the edges of the IBZ

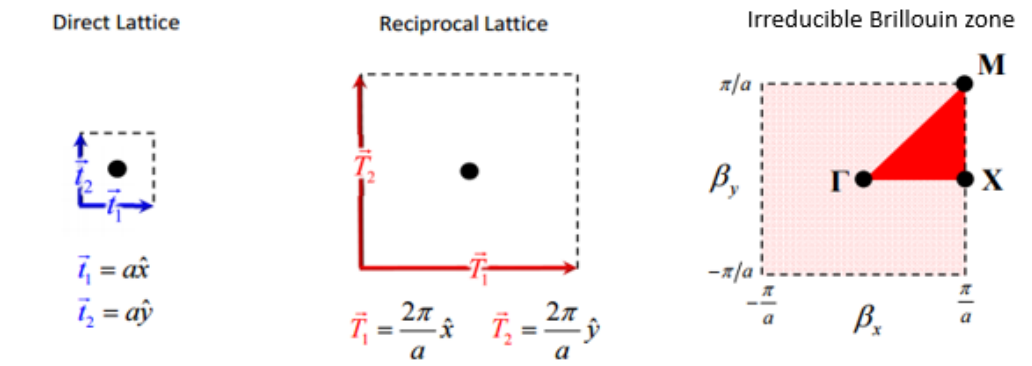

Figure 17: Direct Lattice, Reciprocal lattice, Irreducible Brillouin Zone for 2D periodic square lattice [25]

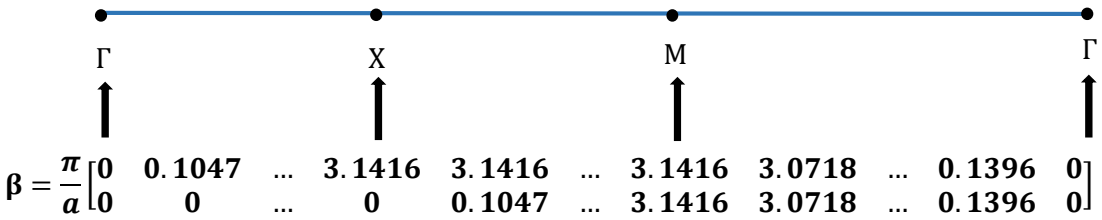

Figure 18: Illustration of choice of Bloch Wave Vectors (origin of the vectors is Γ, and the end is along the edge of the IBZ)

The radius of thee platinum cylinders is set as $r = 1.5 \times 10^{-8} m$, and the period is $a = 3.0 \times 10^{-8} m$. The plasma frequency of platinum is $f_p = 1.244 \times 10^{15} Hz$, $\omega_p = 2\pi v_p = 7.812 \times 10^{15} rad/s$. The collision frequency of Pt in Drude model is $\gamma = 16.73 \times 10^{12} Hz$ [43]. The FDTD cell size is $\Delta x = \Delta y = 3 \times 10^{-10} m$ .The time step, to meet the requirement of the Courant stability criterion, which is $\Delta t = \Delta x/(2c)$, where c is the speed of light in free space. This criterion is stricter than the original one: $\Delta t = \Delta x/(\sqrt{2}c)$. The overall time steps are chosen to be $2^{15} = 32768$.

The dipole sources chosen are varied by modes, In TM^zmode, it is an electric line source, In TM^z mode it is an magnetic line source. The locations are chose in the free-

space region of the 2D simulation domain. The source is chosen as Gaussian pulse within the frequency range of interest. The frequency is normalized by the factor of $a/(2\pi c)$, $\bar{f} = \omega a/(2\pi c) \in [0 \sim 0.5]$, the expression for the Gaussian dipole is :

$$g(t) = e^{-(\frac{t-t_0}{\tau})^2}$$

Where t_0 is the initial time delay, τ controls of the pulse width, the exact pulse width is $B = \frac{1}{\pi\tau}$ (from DC to B), usually$\tau \cong \frac{1}{2B}$, $t_0 \geq 6\tau$.

Dielectric constant of the RuO_2 is set to be 5 and 10 respectively. This assumption results from the procedure of manufacture. The Metal Ru and Pt were co-sputtered to the substrate. The structure of the RuO_2 is amorphous. The conductivity of RuO_2 therefore is neglected. However, the dielectric constant of the RuO_2 is still uncertain. So the dielectric constant of RuO_2 is treated as variable and a parameter sweep is conducted between 5 and 10.

TM^z Mode (Ez, Hx, Hy)

Figure 19 showed the electric and magnetic field components in **TM^z** Mode

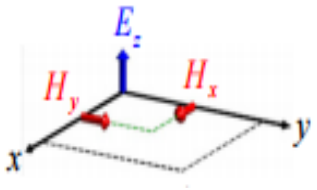

Figure 19: Components of electric and magnetic fields in TM^z Mode

The band diagram in $\mathbf{TM^z}$ Mode with dielectric constant of RuO_2 equal to 5 are presented in figure 20. To make the picture clearly, the lower half of (a) is enlarged and presented in (b)

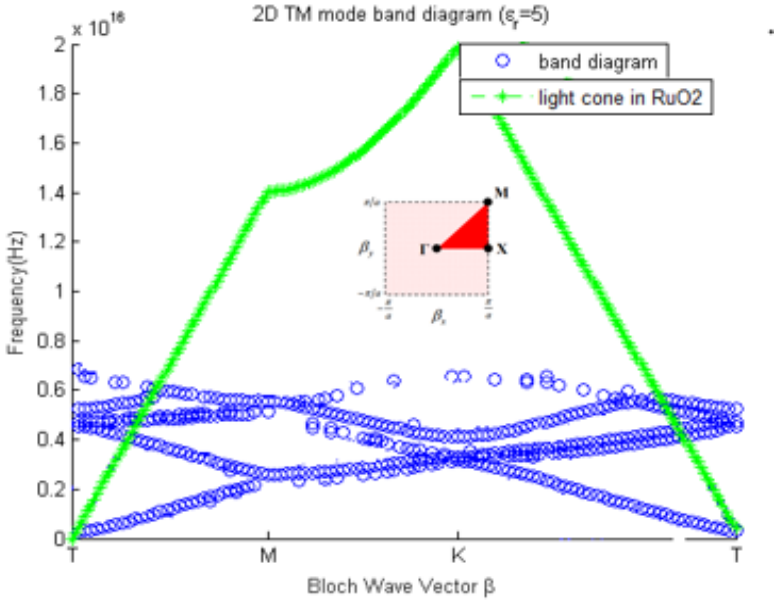

(a)

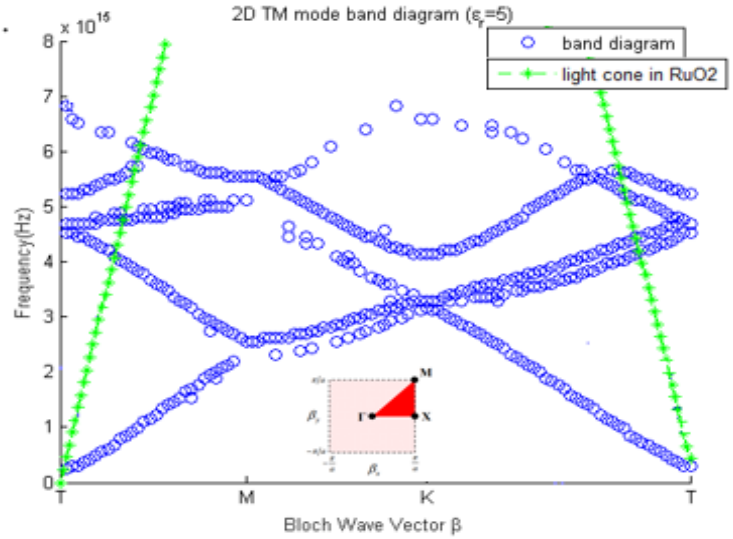

(b)

Figure 20: 2D TM^z mode band diagram ($\varepsilon_{r\_RuO_2}$=5)(a) full light cone (b) partial light cone

Figure 21 shows the band diagram in $\mathbf{TM^z}$ Mode with dielectric constant of RuO_2 equal to 10

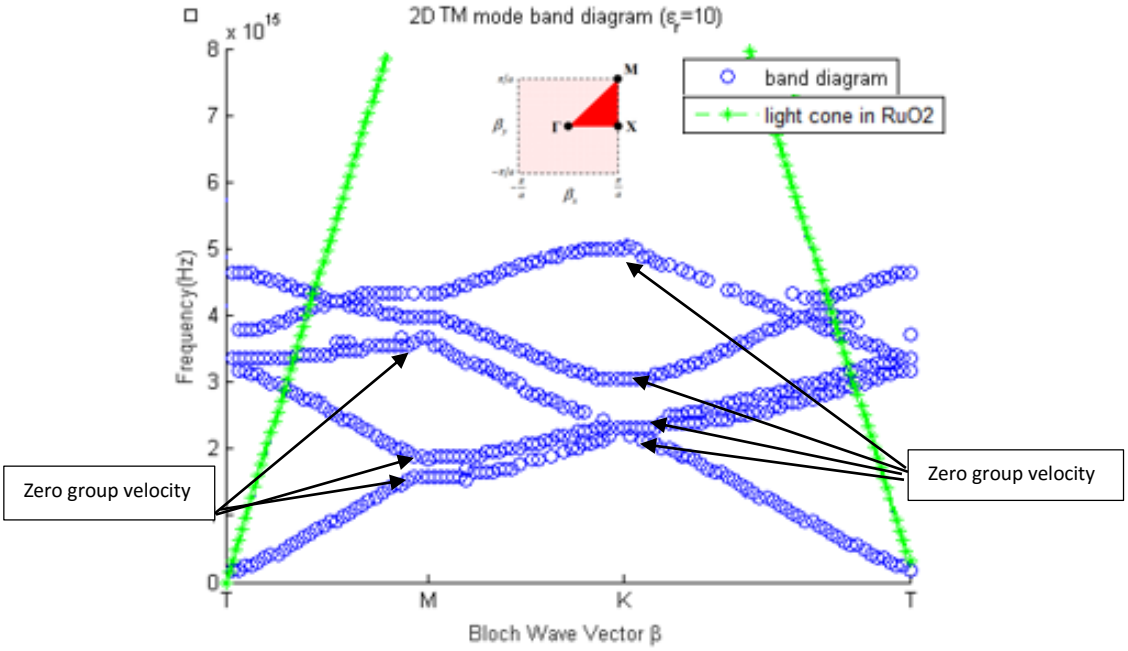

Figure 21: 2D TM^z mode band diagram ($\varepsilon_{r\_RuO_2}$=10)

According to figure 21, the x axis is the Bloch wave vector, which is also the wave vectors of the photons, the y axis is the frequency of the photons. So this band diagram is dispersion curve for the photons. According to Chapter 1, the slope of the tangent line of any point on the despersion curve is the group velocity of the the wave envelope. There are mutiple dots on the curve where the slope are zero, as pointed in the Figure. As for the points correspond to $7.5\times 10^{-6} m/s$, their slopes should be equal to 7.5×10^{-6} . Since this value is extremely small, the points should be very close to point with zero group velocity. Actually, the FDTD algrithm we impemented has minimum freqeuency resolution, and like every numerical alogrithm, it has numerical errors, too. The differnces between points corresponding to $7.5\times 10^{-6}\mathrm{m/s}$ and the ones correspoding to zero group velocity are within the errors of the algrithm and hence are

indistinguishable. However, the errors of the algorithm are not large enough to contradict the existence of the zero group velocity points, so that the zero group velocity points are equivelant to the points with $7.5\times 10^{-6}\mathrm{m/s}$ group velocity. By now we've found mutiple points corresponding to zero group velocity, So we have proven that it is possible that a wave envelope with group velocity of $7.5\times 10^{-6}\mathrm{m/s}$ could propagate through the structure. It could correspond to any points we've identified on the figure.

TE^z Mode (Hz, Ex, Ey fields only)

Figure 22 shows the electric and magnetic field components in **TE^z** Mode

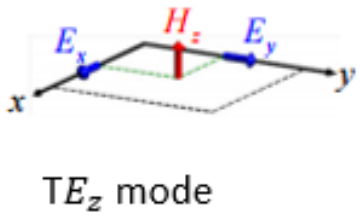

Figure 22: Components of electric and magnetic fields in TE^z Mode

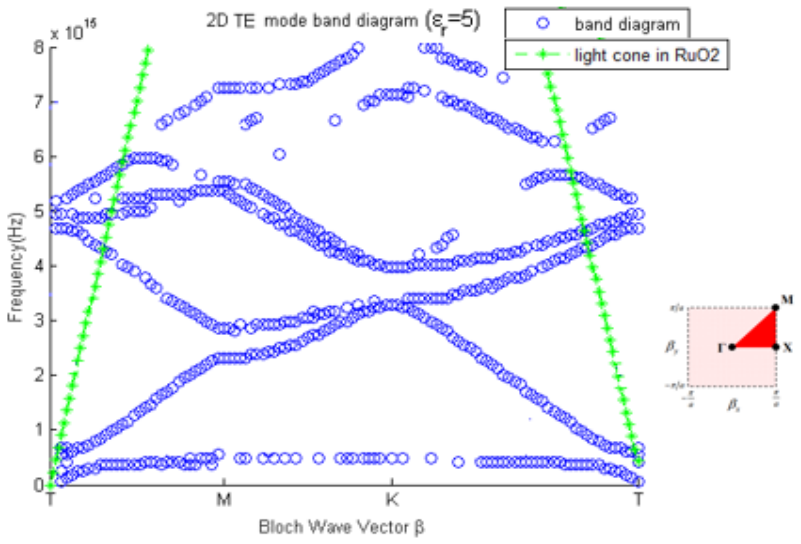

(a)

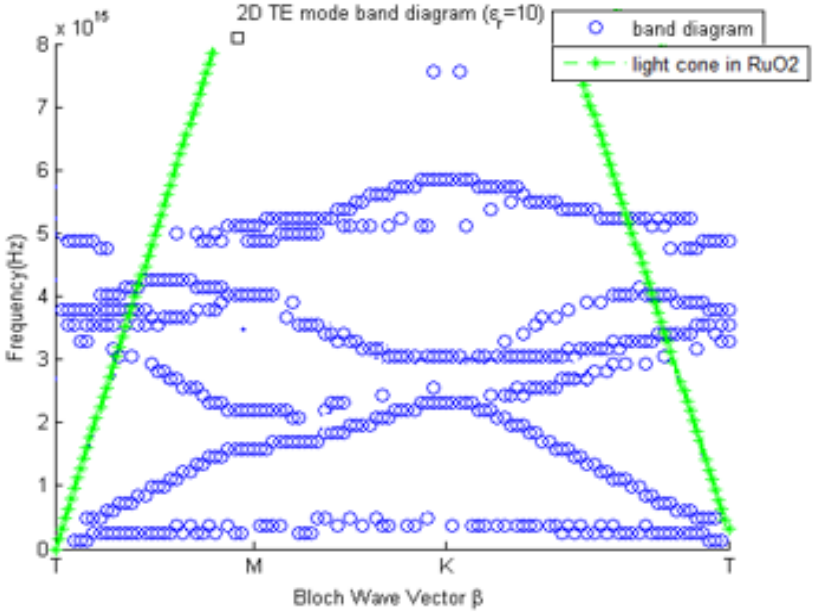

(b)

Figure 23: 2D TE^z mode band diagram ($\varepsilon_{r\_RuO_2}$=5 (a), $\varepsilon_{r\_RuO_2}$=10 (b))

Like figure 21, we could identify multiple zero group velocity points on the dispersion curve where dielectric constant of RuO_2 is set to be 10. This suggest the existence of conditions that will generate a wave envelope with group velocity corresponding to $7.5\times 10^{-6}\mathrm{m/s}$.

Comparing the two dispersion relationships, we could conclude that the general shapes of the dispersion relations are quite similar, and the Bloch wave vectors corresponding to the points of interest are the same while the frequencies are shrink with increasing dielectric constants.

Figure 24 and figure 25 are comparison of the dispersion relationships in different modes with the same dielectric constant of RuO_2.

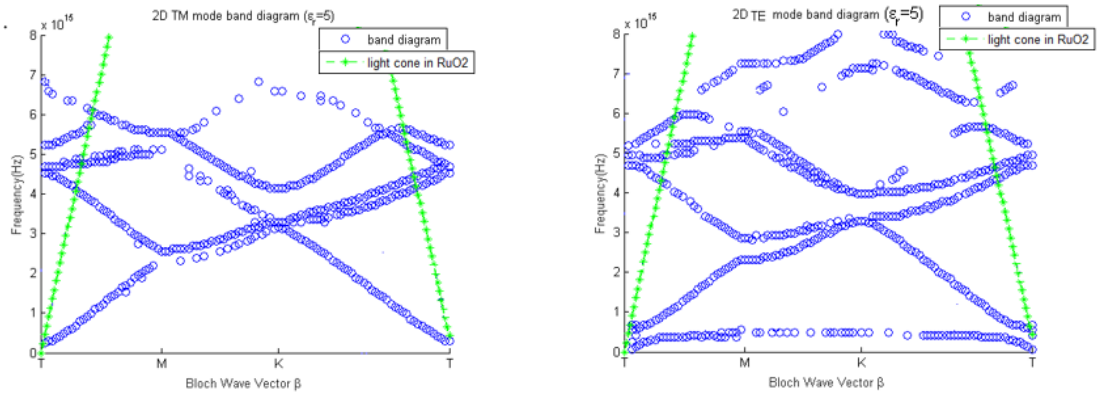

Figure 24: Comparison between different Modes ($\varepsilon_{r\_RuO_2}$=5)

By comparing different modes with the same the dielectric constant of RuO_2, we could find out that the general shapes are different due to different modes, however, the wave vectors of the zero group velocity points are mostly concentrated around M and K.

Similar conclusion can be drawn for the case where dielectric constant of RuO_2 is 10 in figure 25.

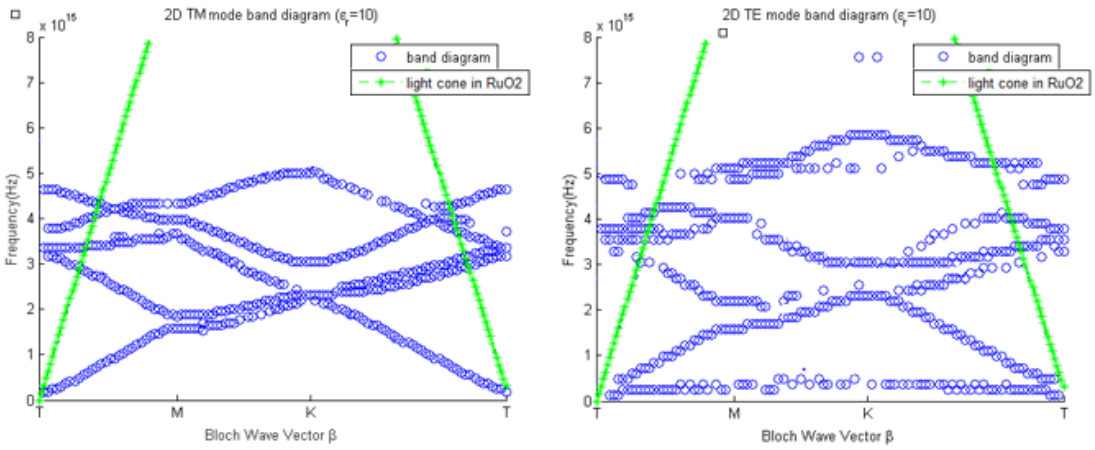

Figure 25: Comparison between different Modes ($\varepsilon_{r\_RuO_2}$=10)

5.2 1-D Band Diagram (Dispersion Diagram)

First of all, we presented the 1D periodic model which has been showed in Chapter 1. We copied it here for easy explanation about the procedure how the unite cell is chosen and constructed, what is the Bloch wave vectors chosen at last.

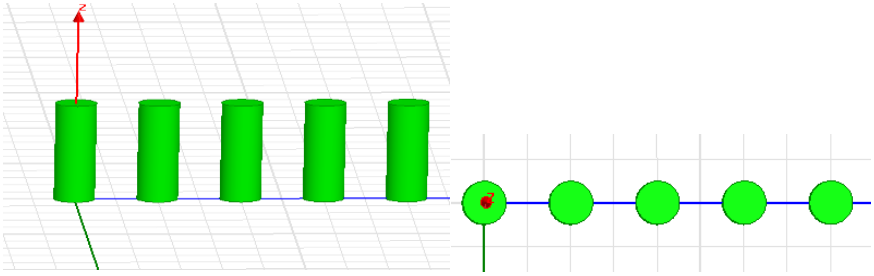

(a) **(b)**

(a) 1D periodic model in 3D view, periodic in x direction and infinitely long in z direction (b) plane 2D view, from above

Figure 26 shows the primitive unit cell constructed in FDTD algorithm.

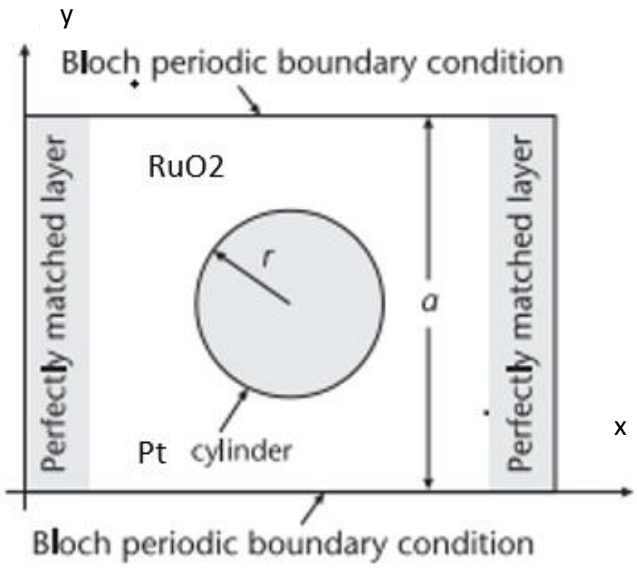

Figure 26: Primitive unit cell constructed in FDTD algorithm

This is a periodical array of Platinum (Pt) cylinder rods along the y direction. The nanorods are si treated as infinitely long in z direction. Since the array is only periodic along the y-direction, PML is applied in the x direcion to absorb outgoing waves, which means the next nano-cylinder is

infinetely far away in the x direction while Bloch periodic boundary conditon is applied in the y direction. The space between the Platinum nanrods and PML is at least a quarter wavelength of interest.

The primitive unit cell of 1D photonic crystal is a line, so is its Brillouin Zone. In Figure 27, The IBZ is from Γ to M. The examples of chosen Bloch vectors are also listed:

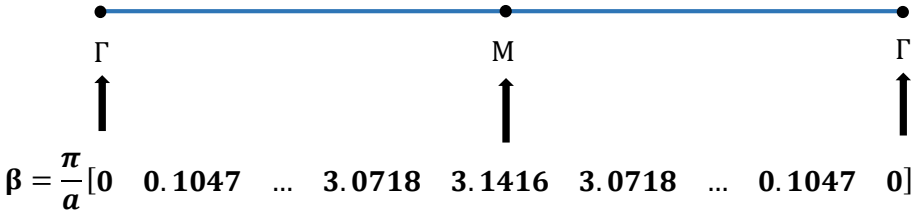

Figure 27: Illustration of choice of Bloch Wave Vectors

TM^z Mode (Ez, Hx, Hy)

The band diagrams of 1D periodic structure in TM^z mode with different dielectric constants are showed in figure 28

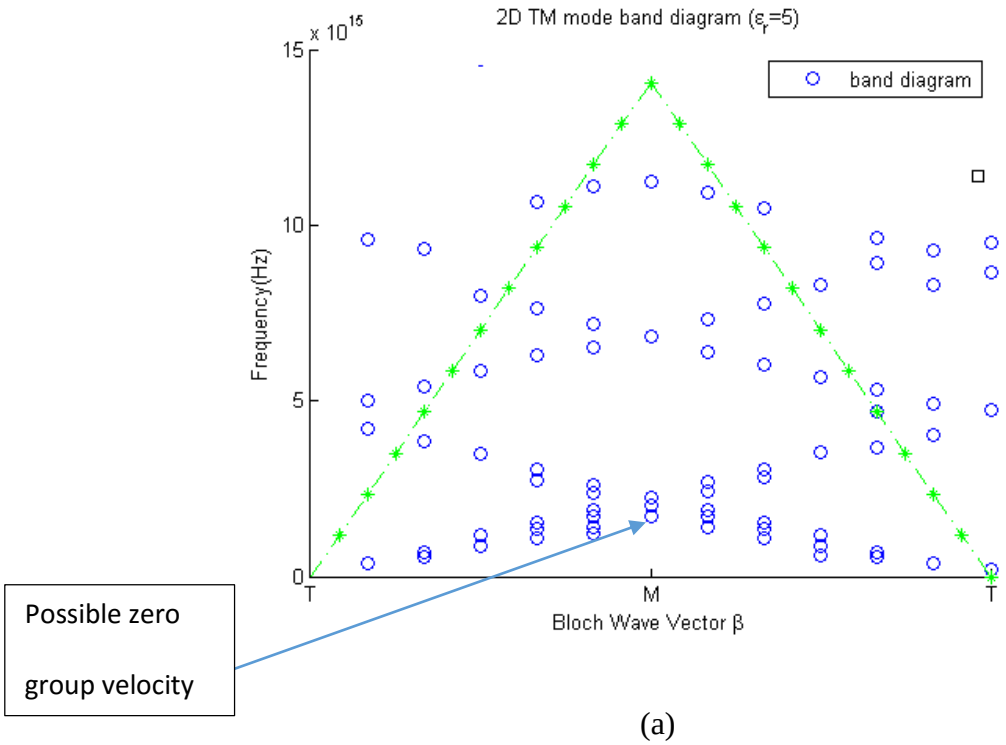

(a)

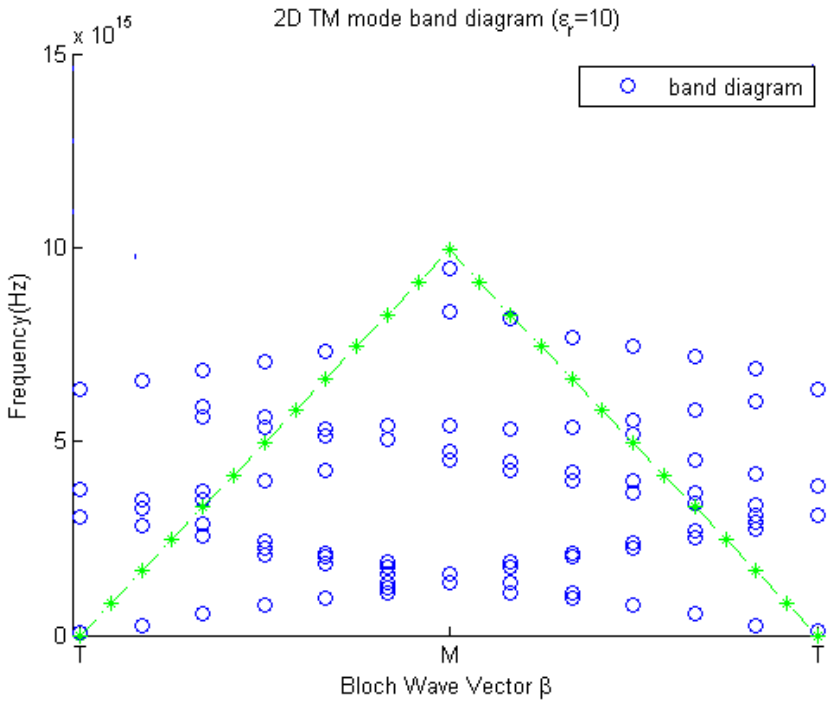

(b)

Figure 28: 2D TM^z mode band diagram ($\varepsilon_{r\_RuO_2}$=5(a) $\varepsilon_{r\_RuO_2}$=10(b))

From Figure 28 (a), we can conclude that the zero group velocity points on the the dispersion curves are achieved by setting Bloch Wave vectors to $\frac{\pi}{a}$, and can only be achieved on the first dispersion curve which is very close to the second one. For higher mode of dispersion curves, the lines intersects at $\frac{\pi}{a}$ with an angle, mathematically, there are no gradients at these points. Since the limits the from left side of the curve and right side of the curve don't converge. A similar conclusion can be draw from Figure 28 (b).

TE^z Mode (Hz, Ex, Ey fields)

The band diagram of 1D periodic structure in TE^z mode with different dielectric constants are showed in figure 29:

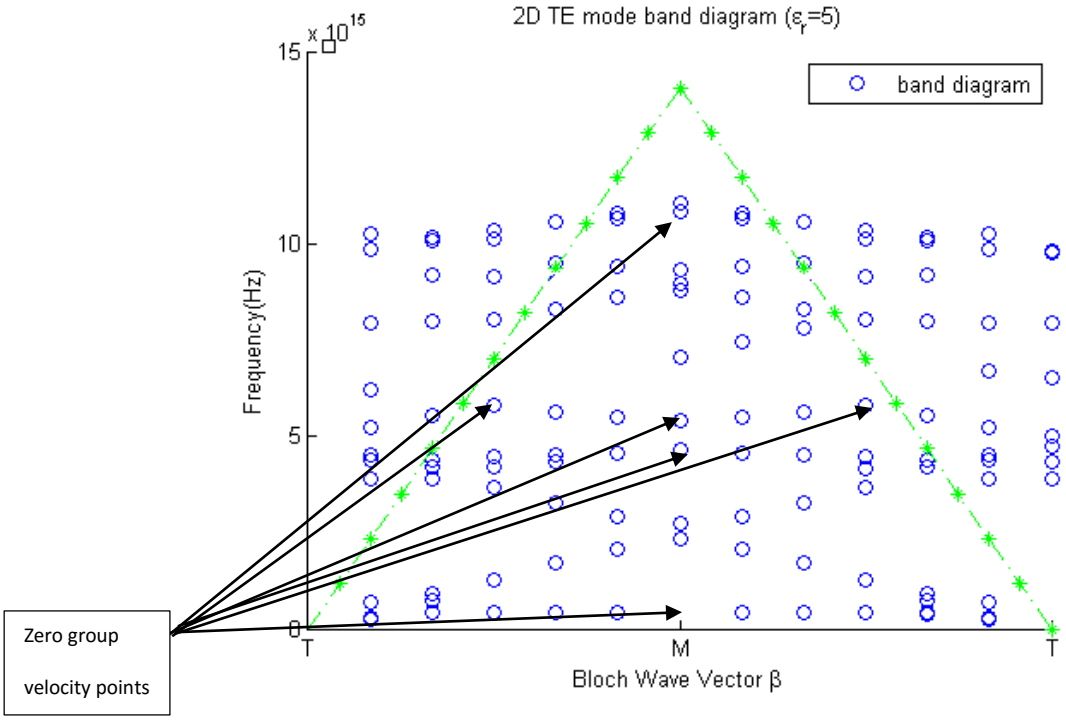

(a)

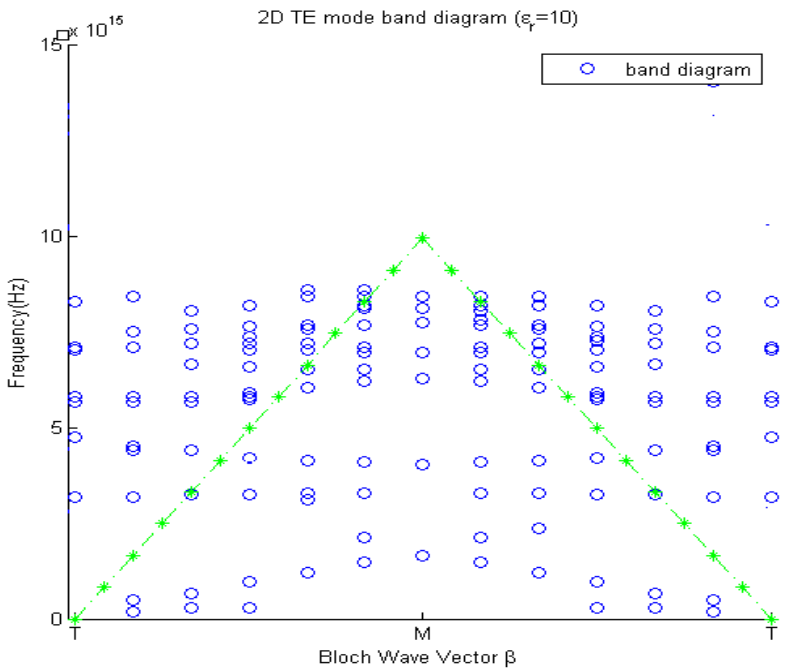

(b)

Figure 29: 2D TE^z mode band diagram ($\varepsilon_{r\_RuO_2}$=5 (a) $\varepsilon_{r\_RuO_2}$=10 (b))

The zero group velocity points are labeled in fig 29 (a), most of them are with wave vectors equal to $\frac{\pi}{a}$, there are two exclusions, on the fifth order of the curve, the zero group velocity points are identified with wave vector roughly equal to $\frac{\pi}{2a}$. For the figure 29 (b), zero group velocity points are identified with wave vector equal to $\frac{\pi}{a}$. The higher order of dispersion relationships are close to each other and cannot be clearly distinguished from each other.

Here are comparisons between dispersion relations with that same dielectric constant, respectively 5 and 10 in figure 30 and 31

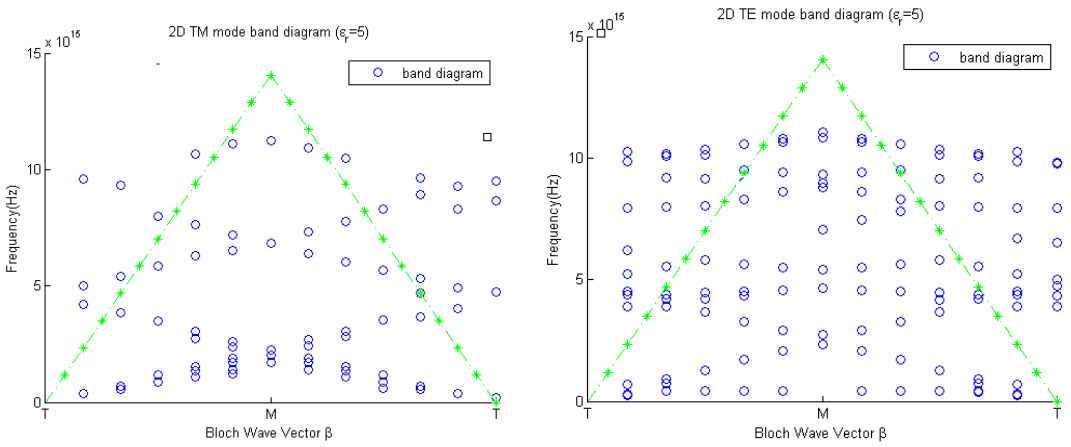

Figure 30: Comparison between different Modes ($\varepsilon_{r\_RuO_2}$=5)

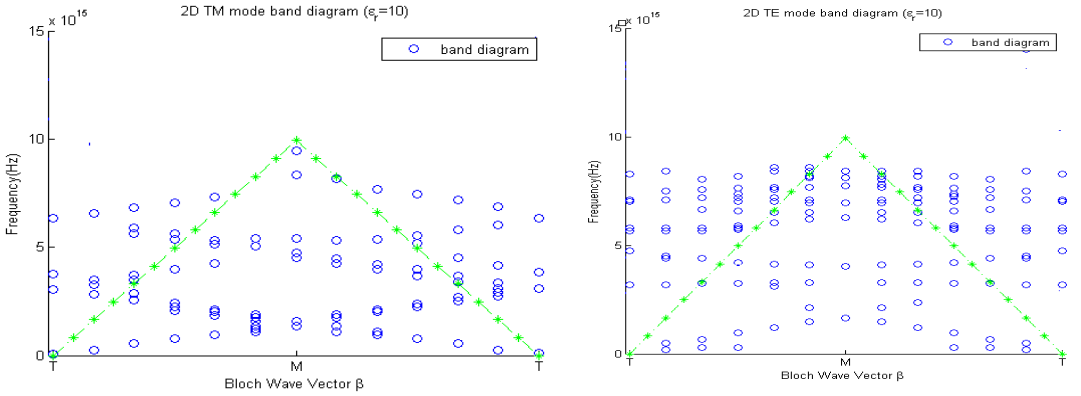

Figure 31: Comparison between different Modes ($\varepsilon_{r\_RuO_2}$=10)

The comparison between different modes with the same dielectric constant of RuO2 shows that the TE^z mode has more zero group velocity points than the TM^z in higher modes, and the wave vectors of zero group velocity points in TE^z modes are not restricted to $\frac{\pi}{a}$.

Conclusion: By simplifying the real structure of the device and creating two geometrical models, we reduce the computational resources required to calculate the

dispersion curve dramatically. After analyzing the dispersion relations in all models and all dielectric constants, it has been found that the conditions sufficient to make group velocity of wave envelope to be zero are abundant, in other words, there are multiple combinations of wave vectors and frequencies to make the group velocity equal to zero. This abundance is much more apparent in the 2D periodic structures in both TM^z and TE^z modes. This suggests that the structure will allow a wave envelope with group velocity of $7.5\times 10^{-6}\mathrm{m/s}$ to propagate through, and the possiblity that it could happen is high.

5.3 Further Discussion

1: The accuracy of the model or in other words, could we identify which point in the set of zero group velocity points would correspond to the wave we observed? The answer is no, we couldn't. To solve this question we would need information that is beyond the videos.

2: Which geometrical and mathmatical model is more accurate, the 2D periodic model or the 1D periodic model? The answer is that the 2D periodic model is more accurate. The substrate is not a cylinder strictly, it is a cuboid before the co-sputterring of Ru and Pt. So more likely the Pt nano rods are on a bouffant cuboid (bouffant rectangular in cross section) whose surfaces are flatter than a cylinder. So this will strengthen the underlying assumption for the 2D periodic model and make the 2D periodic model more realistic.

3: How acurrate is the assumption the Pt nanorods are periodic and if the assumption doesn't hold, what will this thesis prove? The periodicy of the pt nanorods is clear in certain regions of the device as highlightened in figure 32. However, the structure is not strictly periodic. The periodicy is an assumption based on the observation of the TEM pictures, the Pt nanorods likely deviate from the assumed periodic locations assigned in the mathmatical model. The severity of the deviation is unkown. If the overall deviation is slight, The distortion of the dispersion relationship could be treated as a perturbation and hence neglected. If the overall deviation becomes higher, the severely deviated Pt nanorods could be treated as defects in periodic structures. Many researches have done analysis in the effects of defects in Photonic crystal [6,37], the dispersion relationship will be distorted locally somewhere on the curve. The analysis could only be done on a case-by-case basis. Since we have identified mutiple zero group velocity points on the frequency range on both lower and higher modes in 2D case, the complete disappearance of zero group velocity points would be difficult. If the severity of the deviation is so strong that even the least deviated pt nanorods should be teated as defects, then what we are talking about is a totally new structure that my thesis won't explain it.

Here is the picuture where a region with clear periodicy is highlightened:

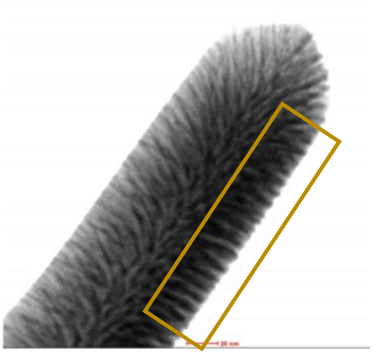

Figure 32: Periodic structures

4 The electron beam will generete electromagnetic wave when it colides with metals, this phenomenon is called **Bremsstrahlung radiation, or breaking radiation.** The radiation is usually within X-ray range. Many dots we've identified are within the X-ray radiation. So the Bremsstrahlung radiation generated by the electron beam in TEM may be the source of the electromagnetic wave that is dispersed through the structure and forms the wave we've identified in the videos.

REFERENCE

[1] Mahmoud Omar, Manasreh. "Introduction to nanomaterials and devices. " Hoboken, N.J.: Wiley, 2010.

[2] Yasitha L. Hewakuruppu, Leonid A. Dombrovsky, Chuyang Chen, Victoria Timchenko, Xuchuan Jiang, Sung Baek, and Robert A. Taylor, "Plasmonic "pump–probe" method to study semi-transparent nanofluids," Appl. Opt. 52 (2013): 6041-6050

[3]Dürig, U.; et al. "Near-field optical scanning microscopy." J. Appl. Phys.59.10 (1986): 3318.

[4] Lukas Novotny, Bert Hecht. Principles of nano-optics. Cambridge, New York: Cambridge University Press, 2006. Web. 11 Feb. 2016

[5] S.Zeng; Baillargeat, Dominique; Ho, Ho-Pui; Yong, Ken-Tye; et al. "Nanomaterials enhanced surface plasmon resonance for biological and chemical sensing applications" . Chemical Society Reviews 43.10(2014): 3426–3452.

[6] John D. Joannopoulos, Steven G. Johnson, Joshua N. Winn, Robert D. Meade. Photonic Crystal, Modeling the flow light. 2nd ed., Princeton, N.J.: Princeton University Press, 2008: 6-43. Print.

[7] S. A. Maier. Plasmonics: Fundamentals and Applications. Springer Science. 2007.

[8] W. Varhue, M. Cross, Thomas Valdez. "RuO2 nanorod coated cathode for the electrolysis of water," International Journal of Hydrogen Energy 37.18 (2012): 13256–13262.

[9] M. Cross, W. Varhue, D. Hitt, E. Adams. "Control of ruthenium oxide nanorod length in reactive sputtering." Nanotechnology 19 (2008): 045611–045615

[10] Leon Brillouin. Wave propagation and group velocity. New York, London, Academic Press, 1960. Print.

[11] "Phase & Group Velocity." Navipedia, . 23 Feb 2012, 11:35 UTC. 7 Apr 2016, 09:06 <http://www.navipedia.net/index.php?title=Phase_%26_Group_Velocity&oldid=11627>.

[12] Born, Max; Wolf, Emil. Principles of Optics. Cambridge: Cambridge University Press, 1999. 14–24.

[13] Charles Kittel. Introduction to solid state physics, 8. Ed, Hoboken, N.J.: Wiley, 2005. Print.

[14] Donald A Neamen. Semiconductor physics and devices: basic principles. 3rd ed. Boston: McGraw-Hill, cop. 2003. Print

[15] J. W. S. Rayleigh. "On the remarkable phenomenon of crystalline reflexion described by Prof. Stokes" , Phil. Mag 26(1888): 256–265,

[16] E. Yablonovitch (1987), "Inhibited Spontaneous Emission in Solid-State Physics and Electronics" , Physical Review Letters 58 (20): 2059–2062

[17] S. John. "Strong localization of photons in certain disordered dielectric superlattices" , Physical Review Letters 58.23 (1987): 2486–2489,

[18] J. Gazalet, S. Dupont, J.C. Kastelik, Q. Rolland, B. Djafari-Rouhani. “A tutorial survey on waves propagating in periodic media: Electronic, photonic and phononic crystals. Perception of the Bloch theorem in both real and Fourier domains.” Wave Motion 50.3 (2013):619-654

[19] Steven G. Johnson, J. D. Joannopoulos. Photonic Crystals: The Road from Theory to Practice Boston:Kluwer. 2002. Print.

[20] Charles W. Myles. Photonic crystal, [PPT document]. Retrieved from Lecture Notes Online Web site:http://www.phys.ttu.edu/~cmyles/Phys4309-5304/Lectures/Photonic%20Crystals.ppt

[21] Wikipedia contributors. "Crystallographic point group." Wikipedia, The Free Encyclopedia. Wikipedia, The Free Encyclopedia, 1 Mar. 2016. Web. 7 Apr. 2016.

[22] Wikipedia contributors. "Bravais lattice." Wikipedia, The Free Encyclopedia. Wikipedia, The Free Encyclopedia, 14 Mar. 2016. Web. 7 Apr. 2016.

[23] Kane Yee. "Numerical solution of initial boundary value problems involving Maxwell's equations in isotropic media". IEEE Transactions on Antennas and Propagation 14.3 (1966): 302–307.

[24] Understanding the Finite-Difference Time-Domain Method, John B. Schneider, www.eecs.wsu.edu/~schneidj/ufdtd, 2010. (Style specified by author).

[25] Raymond C. Rumpf. Electromagnetic Analysis Using Finite-Difference Time-Domain, EE 5390, University of Texas at El Paso, Summer 2014, Retrieved from Web site: http://emlab.utep.edu/ee5390fdtd.htm

[26] Allen Taflove, Susan C. Hagness. Computational Electrodynamics, the finite difference time-domain method. 3rd ed. Artech House. 2005. Print.

[27] J. Berenger. "A perfectly matched layer for the absorption of electromagnetic waves". Journal of Computational Physics 114.2 (1994): 185–200.

[28] CHEW W.C., WEEDON W. “A 3D perfectly matched medium from modified Maxwell’s equations with stretched coordinates.” Microw. Opt. Tech. Lett., 7.13 (1994): 599– 604

[29] C. M. Rappaport. “Perfectly matched absorbing boundary conditions based on anisotropic lossy mapping of space.” IEEE Microwave and Guided Wave Lett., 5.3 (1995): 90–92.

[30] LIU G., GEDNEY S.D. “Perfectly matched leyer for an unconditionally stable three-dimensional ADI-FDTD method.” IEEE Microw. Guid. Wave Lett. 10 (2000): 261–263.

[31] LAZZI G. “Unconditionally stable D-H FDTD formulation with anisotropic pml boundary conditions.” IEEE Microw. Wirel. Compon. Lett. 11.4 (2001): 149– 151

[32] F. L. Teixeira and W. C. Chew. “General closed-form PML constitutive tensors to match arbitrary bianisotropic and dispersive linear media.” IEEE Microwave and Guided Wave Lett. 8.6 (1998): 223–225.

[33] S.D. Gedney. "An anisotropic perfectly matched layer absorbing media for the truncation of FDTD latices". Antennas and Propagation, IEEE Transactions on 44.12 (1996): 1630–1639.

[34] Steven H. Simon. The Oxford Solid State Basics. Oxford: Oxford University Press. 2013

[35] John Singleton. Band theory and electronic properties of solids. New York: Oxford: Oxford University Press. 2001.

[36] Neil Ashcroft; N. David Mermin. Solid State Physics. Saunders College. (1976). pp. 2–6.

[37] Patil, P. B., Pendharker, S. and Shevgaonkar, R. K., “Electrical modeling of photonic crystal defects.” Microw. Opt. Technol. Lett., 54 (2012): 2522–2528.

[38] Raymond C. Rumpf, “Theory of Periodic Structures [PDF document]”, ECE 5322, Retrieved from Lecture Notes Online Web site: http://emlab.utep.edu/ee5390em21/Lecture%207%20--%20Theory%20of%20periodic%20structures.pdf. Web. 7 Apr. 2016.

[39] A. Taflove and S. Hagness, Computational Electrodynamics: The FiniteDifference Time-Domain Method, 3rd ed. Boston, MA: Artech House, 2005, ch. 7.8 Efficient Implementation of UPML in FDTD, pp. 297–322.

[40] A. Taflove and S. Hagness, Computational Electrodynamics: The FiniteDifference Time-Domain Method, 3rd ed. Boston, MA: Artech House, 2005, ch. 16.11 Calculation of Band Structure, pp. 774–784.

[41] Holger Brandsmeier, Kersten Schmidt, Christoph Schwab. “A multiscale hp-FEM for 2D photonic crystal bands.” Journal of Computational Physics 230.2 (2011):349-374

[42] R. Antos, V. Vozda, and M. Veis, "Plane wave expansion method used to engineer photonic crystal sensors with high efficiency," Opt. Express 22 (2014): 2562-2577

[43] M. A. Ordal, Robert J. Bell, R. W. Alexander, L. L. Long, and M. R. Querry, "Optical properties of fourteen metals in the infrared and far infrared: Al, Co, Cu, Au, Fe, Pb, Mo, Ni, Pd, Pt, Ag, Ti, V, and W.." Appl. Opt. 24 (1985): 4493-4499

Appendix A

The constitutive relation between normalized $\widetilde{D}\ and\ \tilde{E}$ is given by:

$$\widetilde{D}(\omega) = \tilde{\varepsilon}_r(\omega) \cdot \tilde{E}(\omega) = \left(1 - \frac{\omega_p^2}{\omega^2 - j\omega\Gamma}\right)\tilde{E}(\omega) = \left(1 + \frac{\omega_p^2}{j\omega\Gamma + (j\omega)^2}\right)\tilde{E}(\omega)$$

Where the normalization is done by: $\vec{\tilde{E}} = \frac{1}{\eta_0}\vec{E}$ $\eta_0 = \sqrt{\frac{\mu_0}{\varepsilon_0}}$ $\vec{\widetilde{D}} = \frac{1}{\sqrt{\mu_0\varepsilon_0}} = \frac{1}{c_0}\vec{D}$

After the normalization, the constitutive takes the form as above, the $\tilde{\varepsilon}_0$ is omitted.

Multiple both sides of the equation by $(j\omega\Gamma + (j\omega)^2)$:

$$(j\omega\Gamma + (j\omega)^2)\widetilde{D}(\omega) = (j\omega\Gamma + (j\omega)^2)\tilde{E}(\omega) + \omega_p^2\tilde{E}(\omega)$$

$$\Gamma\frac{\partial\widetilde{D}(\mathrm{t})}{\partial t} + \frac{\partial^2\widetilde{D}(\mathrm{t})}{\partial t^2} = \Gamma\frac{\partial\tilde{E}(\mathrm{t})}{\partial t} + \frac{\partial^2\tilde{E}(\mathrm{t})}{\partial t^2} + \omega_p^2\tilde{E}(t)$$

$$\Gamma\frac{\partial\widetilde{D}(\mathrm{t})}{\partial t} \longrightarrow \Gamma\frac{\widetilde{D}(\mathrm{t})\big|_{t+\Delta t} - \widetilde{D}(\mathrm{t})\big|_{t-\Delta t}}{2\Delta t}$$

$$\frac{\partial^2\widetilde{D}(\mathrm{t})}{\partial t^2} \longrightarrow \frac{\frac{(\widetilde{D}(\mathrm{t})\big|_{t+\Delta t} - \widetilde{D}(\mathrm{t})\big|_{t})}{\Delta t} - \frac{(\widetilde{D}(\mathrm{t})\big|_{t} - \widetilde{D}(\mathrm{t})\big|_{t-\Delta t})}{\Delta t}}{\Delta t}$$

$$= \frac{(\widetilde{D}(\mathrm{t})\big|_{t+\Delta t} - 2\widetilde{D}(\mathrm{t})\big|_{t} + \widetilde{D}(\mathrm{t})\big|_{t-\Delta t})}{\Delta t}$$

$$\Gamma\frac{\partial\tilde{E}(\mathrm{t})}{\partial t} \longrightarrow \Gamma\frac{\tilde{E}(\mathrm{t})\big|_{t+\Delta t} - \tilde{E}(\mathrm{t})\big|_{t-\Delta t}}{2\Delta t}$$

$$\frac{\partial^2 \tilde{E}(\mathrm{t})}{\partial t^2} \longrightarrow \frac{\frac{(\tilde{E}(\mathrm{t})|_{t+\Delta t} - \tilde{E}(\mathrm{t})|_t)}{\Delta t} - \frac{(\tilde{E}(\mathrm{t})|_t - \tilde{E}(\mathrm{t})|_{t-\Delta t})}{\Delta t}}{\Delta t}$$

$$= \frac{(\tilde{E}(\mathrm{t})|_{t+\Delta t} - 2\tilde{E}(\mathrm{t})|_t + \tilde{E}(\mathrm{t})|_{t-\Delta t})}{\Delta t}$$

$$\omega_p^2 \tilde{E}(t) \longrightarrow \frac{\tilde{E}(\mathrm{t})|_{t+\Delta t} + 2\tilde{E}(\mathrm{t})|_t + \tilde{E}(\mathrm{t})|_{t-\Delta t}}{4\Delta t}$$

Reorganize the equations, the update coefficients and equations are:

$$m_{Ex0} = 4 + 2\Gamma\Delta t + \omega_p^2 \Delta t^2$$

$$m_{Ex1} = \frac{1}{m_{Dx0}}(4 + 2\Gamma\Delta t)$$

$$m_{Ex2} = -\frac{8}{m_{Dx0}}$$

$$m_{Ex3} = \frac{1}{m_{Dx0}}(4 - 2\Gamma\Delta t)$$

$$m_{Ex4} = \frac{1}{m_{Dx0}}(8 - 2\omega_p^2 \Delta t^2)$$

$$m_{Ex5} = \frac{1}{m_{Dx0}}(2\Gamma\Delta t - 4 - \omega_p^2 \Delta t^2)$$

$$\tilde{E}_x\big|_{t+\Delta t}^{i,j,k} = (m_{Ex1}\big|^{i,j,k})\widetilde{D}_x\big|_{t+\Delta t}^{i,j,k} + (m_{Ex2}\big|^{i,j,k})\widetilde{D}_x\big|_{t}^{i,j,k} + \left(m_{Ex3}\big|^{i,j,k}\right)\widetilde{D}_x\big|_{t-\Delta t}^{i,j,k}$$
$$+ \left(m_{Ex4}\big|^{i,j,k}\right)\tilde{E}_x\big|_{t}^{i,j,k} + \left(m_{Ex5}\big|^{i,j,k}\right)\tilde{E}_x\big|_{t-\Delta t}^{i,j,k}$$

Since the material we simulated is isotopic, so the update coefficients for $\tilde{E}_y$ *and* $\tilde{E}_z$ are identical. Replace the $\widetilde{D}_x$ and $\tilde{E}_x$ with corresponding components and will get the updated equations for $\tilde{E}_y\big|_{t+\Delta t}^{i,j,k}$ and $\tilde{E}_z\big|_{t+\Delta t}^{i,j,k}$

Appendix B

```
%TE mode 2D-FDTD algorithm
%isotopic linear dispersive material
%Drude model incorporated
%electic field nomalized
%UPML for two directions
%Band Diagram calculation
%Square lattice


clear all;
%*********************************************************************
*
%     Fundamental constants
%*********************************************************************
*

cc=2.99792458e8;            %speed of light in free space
muz=4.0*pi*1.0e-7;          %permeability of free space
epsz=1.0/(cc*cc*muz);       %permittivity of free space

%*********************************************************************
*
%     Grid parameters parameters and other parameters
%*********************************************************************
*
a=3e-8;                          % Lattice dimension for square lattice
Nx=100;                          % grid number in x direction
Ny=100;                          % grid number in y direction
dx=a/Nx;                         % x increment
dy=a/Nx;                         % y increment
fx=cc/a/2;
tao=0.1/fx;                      % width of Gaussian wave source
dt1=tao/10;
dt2=dx/2/cc;                     % Courant stability criterion
dt=min(dt1,dt2);                 % calculation of time step
```

```
steps=2^15;                         % How many time will be simulated
x=linspace(dx,Nx*dx,Nx);
y=linspace(dy,Ny*dy,Ny);            % initialize x and y coordinate
WidthPML=10;                        % thickness of PML region


num_rod_x=1;
num_rod_y=1;
ratio=0.25;                         % paramter used to intialize
                                    % the field matrix

[BEX,BEY,BHZ,DEX,DEY,D]=nanocylinder_2XD_7(Nx,Ny,dx,dy,num_rod_x,num_ro
d_y,ratio);
                                    % call function to initialize the field
                                    % matrix
%*************************************************************************
*
%     Compute source
%*************************************************************************
*
fmax =1/dt;
t    =[0:steps-1]*dt;               %time axis
t0   =5*tao;                        %time delay of Gaussian wave
Hsrc =10*exp(-((t-t0)/tao).^2);     %H field source
%*************************************************************************
*
%     Initialize Material parameters
%     & Initialize electric and magnetic field
%     & Initialize curl arrays
%     & Initialize intergration arrays
%*************************************************************************
*

Erxx=(ones(Nx,Ny)-BEX)*10+BEX*1;            %array of permittivity
Erxx
Eryy=(ones(Nx,Ny)-BEY)*10+BEY*1;            %array of permittivity
Eryy
Urzz=ones(Nx,Ny);             %array of permeability Urzz

Hz=zeros(Nx,Ny);              %array Hx Hy Dz and Ez are initialized as
0
Ex=zeros(Nx,Ny);
Ey=zeros(Nx,Ny);
Dx=zeros(Nx,Ny);
Dy=zeros(Nx,Ny);

CHx=zeros(Nx,Ny);             %array of curl of E and H initialized as
0
CHy=zeros(Nx,Ny);
CEz=zeros(Nx,Ny);

IHz=zeros(Nx,Ny);             %array of integration
```

```
ICHx=zeros(Nx,Ny);
ICHy=zeros(Nx,Ny);

Ex00=zeros(Nx,Ny);              %Electrical field inside the circle
Ex01=zeros(Nx,Ny);
Ey00=zeros(Nx,Ny);
Ey01=zeros(Nx,Ny);

Dxn_1=zeros(Nx,Ny);             %D at the time of n in tne update
equations
                                %and Dx,Dy,Dz will represent the D at
time
                                %of n+1 in the update equations
Dxn_2=zeros(Nx,Ny);             %D at the time of n-1 in the update
equations
Dyn_1=zeros(Nx,Ny);
Dyn_2=zeros(Nx,Ny);

Exn_1=zeros(Nx,Ny);              % similar with D
Exn_2=zeros(Nx,Ny);
Eyn_1=zeros(Nx,Ny);
Eyn_2=zeros(Nx,Ny);

%**********************************************************************
*
%     Compute PML parameters
%**********************************************************************
*

%compute sigx and sigy on 2*grid
%compute PML parameters

NPML=[0 0 0 0];          %in sequence are NXLO,NXHI,NYLO,NYHI
                         %[0 0 0 0] means non-PML situation

Nx2=2*Nx;
Ny2=2*Ny;

sigx=zeros(Nx2,Ny2);
for nx=1:2*NPML(1);
    nx1=2*NPML(1)-nx+1;
    sigx(nx1,:)=(0.5*epsz/dt)*(nx/2/NPML(1))^3;
end
for nx=1:2*NPML(2)
    nx1=Nx2-2*NPML(2)+nx;
    sigx(nx1,:)=(0.5*epsz/dt)*(nx/2/NPML(2))^3;
end

sigy=zeros(Nx2,Ny2);
for ny=1:2*NPML(3);
    ny1=2*NPML(3)-ny+1;
    sigy(:,ny1)=(0.5*epsz/dt)*(ny/2/NPML(3))^3;
```

```
end
for ny=1:2*NPML(4);
    ny1=Ny2-2*NPML(4)+ny;
    sigy(:,ny1)=(0.5*epsz/dt)*(ny/2/NPML(4))^3;
end

%sigx=sigx*10;
%sigy=sigy*10;

%*************************************************************************
*
%     Compute update efficients for D and H
%*************************************************************************
*

sigxDx=sigx(2:2:Nx2,1:2:Ny2);          %now sigxDx and sigxDy are
fictious
sigyDx=sigy(2:2:Nx2,1:2:Ny2);          %sigma is at the location of Dx
mDx0=(1/dt)+sigyDx/(2*epsz);
mDx1=((1/dt)-sigyDx/(2*epsz))./mDx0;
mDx2=cc./mDx0;
mDx3=((cc*dt/epsz)*sigxDx)./mDx0;


sigxDy=sigx(1:2:Nx2,2:2:Ny2);          %now sigyDx and sigyDy are
fictious
sigyDy=sigy(1:2:Nx2,2:2:Ny2);          %sigma is at the location of Dy
mDy0=(1/dt)+sigxDy/(2*epsz);
mDy1=((1/dt)-sigxDy/(2*epsz))./mDy0;
mDy2=cc./mDy0;
mDy3=((cc*dt/epsz)*sigyDy)./mDy0;


sigxHz=sigx(2:2:Nx2,2:2:Ny2);          % sigxHz sigyHz are sigma at the
sigyHz=sigy(2:2:Nx2,2:2:Ny2);          % the location of Hz
mHz0=(1/dt)+(sigxHz+sigyHz)/(2*epsz)+sigxHz.*sigyHz*dt/4/(epsz^2);
mHz1=(1/dt)-(sigxHz+sigyHz)/(2*epsz)-sigxHz.*sigyHz*dt/4/(epsz^2);
mHz1=mHz1./mHz0;
mHz2=-1*cc./Urzz./mHz0;
mHz4=(-1*dt/(epsz^2))*sigxHz.*sigyHz./mHz0;

%*************************************************************************
*
%     Compute update efficients for E
%*************************************************************************
*
% Drude model parameters
Wp_1=7.816e15;             %plasmon frequecy rad/s
%Wp_1=0;                   %set wp_1=0 when testing non-dispersive
material
g_1=1.673e13;              %collision frequecy Hz
```

```
%g_1=0;                    %set g_1=0 when testing non-dispersive
material
wpex=Wp_1*BEX;
wpey=Wp_1*BEY;
gex=g_1*BEX;
gey=g_1*BEY;

mEx0=4*Erxx+2*Erxx.*gex*dt+(wpex.^2)*(dt^2);%epsinf is a matrix size of
Nx, Ny,Nz
mEx00=mEx0;
mEx1=((2*gex*dt+4)./mEx0);
mEx2=((4-2*gex*dt)./mEx0);
mEx3=(-8./mEx0);
mEx4=(-(4*Erxx-2*Erxx.*gex*dt+(wpex.^2)*(dt^2))./mEx0);
mEx5=((8*Erxx-2*(wpex.^2)*(dt^2))./mEx0);

mEy0=4*Eryy+2*Eryy.*gey*dt+(wpey.^2)*(dt^2);%epsinf is a matrix size of
Nx, Ny,Nz
mEy00=mEy0;
mEy1=((2*gey*dt+4)./mEy0);
mEy2=((4-2*gey*dt)./mEy0);
mEy3=(-8./mEy0);
mEy4=(-(4*Eryy-2*Eryy.*gey*dt+(wpey.^2)*(dt^2))./mEy0);
mEy5=((8*Eryy-2*(wpey.^2)*(dt^2))./mEy0);




%%**********************************************************************
**
%     2D FDTD Main Loop with band calculation unit
%**********************************************************************
*
dots=106;                                % number of bloch wave vector
band=6;                                  % number of bands ploted
DP1=zeros(dots,band);
DP2=zeros(dots,band);
for multi=1:4                            % calculate the same band
diagram
                                         % multiple time for comparison
and
                                         % elimination of random errors
%Calculate 100 random recording points

non=find(D);                             %Indices for the free space
Midindr=randi(length(non),100,1);        %choose 100 points in free
space
INDr=non(Midindr);                       %indices of the 100 points in D
matrix
sod=[100,120];                           %size  of D matrix
[Ired,Jred]=ind2sub(sod,INDr);           %subscript of 100 record points
```

```
% claculate 10 random source points
Midinds=randi(length(non),10,1);        %choose 10 points in free space
INDs=non(Midinds);                      %indices of the 100 points in D
matrix
sod=[100,120];                          %size  of D matrix
[Isrc,Jsrc]=ind2sub(sod,INDs);          %subscript of 100 record points


dispersion1=zeros(dots,band);
dispersion2=zeros(dots,band);

f =(1/dt*(0:steps/2-1)/steps);

for s=1:dots
%*************************************************************************
*
%     Reinitialize the fields each time to recalculate band diagram
%*************************************************************************
*

Erxx=(ones(Nx,Ny)-BEX)*10+BEX*1;             %array of permittivity
Erxx
Eryy=(ones(Nx,Ny)-BEY)*10+BEY*1;             %array of permittivity
Eryy
Urzz=ones(Nx,Ny);              %array of permeability Urzz

Hz=zeros(Nx,Ny);               %array Hx Hy Dz and Ez are initialized as
0
Ex=zeros(Nx,Ny);
Ey=zeros(Nx,Ny);
Dx=zeros(Nx,Ny);
Dy=zeros(Nx,Ny);

CHx=zeros(Nx,Ny);              %array of curl of E and H initialized as
0
CHy=zeros(Nx,Ny);
CEz=zeros(Nx,Ny);

IHz=zeros(Nx,Ny);              %array of integration
ICHx=zeros(Nx,Ny);
ICHy=zeros(Nx,Ny);

Ex00=zeros(Nx,Ny);             %Electrical field inside the circle
Ex01=zeros(Nx,Ny);
Ey00=zeros(Nx,Ny);
Ey01=zeros(Nx,Ny);

Dxn_1=zeros(Nx,Ny);
Dxn_2=zeros(Nx,Ny);
Dyn_1=zeros(Nx,Ny);
Dyn_2=zeros(Nx,Ny);
```

```
Exn_1=zeros(Nx,Ny);             % similar as D
Exn_2=zeros(Nx,Ny);
Eyn_1=zeros(Nx,Ny);
Eyn_2=zeros(Nx,Ny);


numvx=106;
numvy=106;
[Bx,By]=newvector(numvx,numvy); %call function to calculate bloch wave
vector

Sx=Nx*dx;
Sy=Ny*dy;
bx=Bx(s)/Sx;
by=By(s)/Sy;
%Calculate Phase Across Grid
phix=exp(-1i*bx*Sx);
phiy=exp(-1i*by*Sy);



%MAIN LOOP
for T=1:steps

        for o=1:10
        Hz(Isrc(o),Jsrc(o))=Hz(Isrc(o),Jsrc(o))+Hsrc(T);
        end
     %compute CEz
        for ny=1:Ny-1
            for nx=1:Nx-1
                CEz(nx,ny)=(Ey(nx+1,ny)-Ey(nx,ny))/dx...
                            -(Ex(nx,ny+1)-Ex(nx,ny))/dy;
            end
            CEz(Nx,ny)=(phix*Ey(1,ny)-Ey(Nx,ny))/dx...
                        -(Ex(Nx,ny+1)-Ex(Nx,ny))/dy;
        end
        for nx=1:Nx-1
            CEz(nx,Ny)=(Ey(nx+1,Ny)-Ey(nx,Ny))/dx...
                        -(phiy*Ex(nx,1)-Ex(nx,Ny))/dy;
        end
        CEz(Nx,Ny)=(phix*Ey(1,Ny)-Ey(Nx,Ny))/dx...
                    -(phiy*Ex(Nx,1)-Ex(Nx,Ny))/dy;   %Bloch periodic
                                                     %boundary
conditions

    %Update H Integration

    IHz=IHz+Hz;

    %Update H from curl of E
```

```
 Hz=mHz1.*Hz+mHz2.*CEz+mHz4.*IHz;


    %compute CHx
    for nx=1:Nx
        CHx(nx,1)=(Hz(nx,1)-conj(phiy)*Hz(nx,Ny))/dy;
        for ny=2:Ny
        CHx(nx,ny)=(Hz(nx,ny)-Hz(nx,ny-1))/dy;
        end
    end                                                 %Bloch periodic
                                                        %boundary conditions

    %compute CHy
    for ny=1:Ny
        CHy(1,ny)=-(Hz(1,ny)-conj(phix)*Hz(Nx,ny))/dx;
        for nx=2:Nx
        CHy(nx,ny)=-(Hz(nx,ny)-Hz(nx-1,ny))/dx;
        end
    end                                                  %Bloch periodic
                                                         %boundary
conditions



    %Update D Integration
            ICHx=ICHx+CHx;
            ICHy=ICHy+CHy;

    %Update Dz
            Dx=mDx1.*Dx+mDx2.*CHx+mDx3.*ICHx;
            Dy=mDy1.*Dy+mDy2.*CHy+mDy3.*ICHy;

    %Update E from D


Ex=mEx1.*Dx+mEx2.*Dxn_2+mEx3.*Dxn_1+mEx4.*Exn_2+mEx5.*Exn_1;

Ey=mEy1.*Dy+mEy2.*Dyn_2+mEy3.*Dyn_1+mEy4.*Eyn_2+mEy5.*Eyn_1;

            Dxn_2=Dxn_1;                    %update Dn and Dn-1
            Dxn_1=Dx;

            Dyn_2=Dyn_1;
            Dyn_1=Dy;

            Exn_2=Exn_1;                   %update En and En-1
            Exn_1=Ex;

            Eyn_2=Eyn_1;
            Eyn_1=Ey;
```

```
            %Update Fourier Transforms
            for q=1:100
                rx=Ired(q);
                ry=Jred(q);
                Ex_record(q,T)=Ex(rx,ry);
                Ey_record(q,T)=Ey(rx,ry);
            end

            Ex_p(1,T)=Ex(Isrc(1),Jsrc(1)+1);
            Ey_p(1,T)=Ey(Isrc(1),Jsrc(1)+1);

            f1 =log10(fmax*(0:T/2-1)/T);
            f2 =log10(1/dt*(0:T/2-1)/T);
            f3 =log10(1/dt*(0:steps/2-1)/steps);


%**************************************************************************
*
%     Plot field, PSD and band diagram
%**************************************************************************
*
if mod(T,2^13)==0;
rsteps=num2str(T);
                E=Ex_record.*Ex_record+Ey_record.*Ey_record;
                FFT_record=fft(E,T,2);
            for q=1:100
                FFTP=FFT_record(q,:);
                FFTT=FFTT+FFTP;
            end

            Ep=Ex_p.*Ex_p+Ey_p.*Ey_p;
            FFTQ=fft(Ep);
            Qr=(abs(FFTT(1:T/2)));
            Qr2=(abs(FFTQ(1:T/2)));
            Qr3=(abs(fft(Hsrc)));
            [pks,locs]=findpeaks(Qr,'SortStr','descend');
            [pks2,locs2]=findpeaks(Qr2,'SortStr','descend');
            %[pks,locs]=findpeaks(Qr);
            %[pks2,locs2]=findpeaks(Qr2);

figure(21),imagesc(abs(Hz'));
colorbar;
%caxis([-0.1,0.1]);
caxis auto
axis image; axis xy;
axis off;
title(['Hz at time step = ',rsteps]);
shading interp ;

figure(31)
```

```
subplot(3,1,1)
plot(f1,Qr);
hold on;
plot(f1(locs),pks+0.05,'k^','markerfacecolor',[1 0 0]);
hold off;
title(['Overall PSD at time step = ',rsteps]);

subplot(3,1,2)
plot(f2,Qr2);
hold on;
plot(f2(locs2),pks2+0.05,'k^','markerfacecolor',[1 0 0]);
hold off;
title(['One point near source PSD at time step = ',rsteps]);

subplot(3,1,3)
plot(f3,Qr3(1:steps/2));
title(['PSD of source at time step = ',rsteps]);
FFTT=zeros(1,T+1);
else
FFTT=zeros(1,T+1);
end

end

% identify eigen-frequency
dispersion1(s,:)=f(locs(1:band));
dispersion2(s,:)=f(locs2(1:band));
figure(4+multi)
hold on;
% plot first few band of band diagram
plot(ones(1,band)*s,dispersion1(s,1:band),'o','LineWidth',0.01);

end
% record all the eigen-frequency
DP1=cat(3,dispersion1,DP1);
DP2=cat(3,dispersion2,DP2);

clear Hz_record;
clear Hz_p
end



%%%%%%%%%%%%%%%%%%%%%%%%%%%%%%%%%%%%%%%%%%%%%%%%%%%%%%%%%%%%%%%%%%%%%%%%%%%%
%Function called in the previous algorithm for the calculation of field
%matrix


function[BEX,BEY,BHZ,DEX,DEY,D]=nanocylinder_2XD_7(Nx,Ny,dx,dy,num_rod_
x,num_rod_y,ratio)
%calculate the field matrix with 2X grid technique
```

```
N2X=Nx*2;
N2Y=Ny*2;
xa=[0:N2X-1];
ya=[0:N2Y-1];

a2=N2X/num_rod_x;
r2=a2*ratio;
center_x2=zeros(1,num_rod_x);
center_y2=zeros(1,num_rod_y);

for i=1:num_rod_x
    center_x2(i)=a2/2+(i-1)*a2;
end

for j=1:num_rod_y
    center_y2(j)=a2/2+(j-1)*a2;
end

A=zeros(N2X,N2Y);
[Y2,X2]=meshgrid(ya,xa);
B=A;
for nx=1:num_rod_x
    for ny=1:num_rod_y
        A=(((X2-center_x2(nx)).^2+(Y2-center_y2(ny)).^2)<=r2^2);
        B=B+A;
    end
end



BEX=B(2:2:N2X,1:2:N2Y);
BEY=B(1:2:N2X,2:2:N2Y);
BEZ=B(1:2:N2X,1:2:N2Y);
BHX=B(1:2:N2X,2:2:N2Y);
BHY=B(2:2:N2X,1:2:N2Y);
BHZ=B(2:2:N2X,2:2:N2Y);

%PML region
xa1=[0:Nx-1];
ya1=[0:Ny-1];
[Y,X]=meshgrid(ya1,xa1);
C=zeros(Nx,Ny);
C=((Y<0)|(Y>=Ny));

% calculate non-metal space
TTB=BEX+BEY;
TB=(TTB>=1);
DEX=ones(Nx,Ny);
DEY=ones(Nx,Ny);
D  =ones(Nx,Ny);
DEX=DEX-C-BEX;
DEY=DEY-C-BEY;
D  =D-C-TB;
```

```
% plot the device
figure(1)
imagesc(ya,xa,B);
colorbar;
figure(11)
subplot(3,1,1)
imagesc(ya1,xa1,D);
colorbar;
axis equal tight;
subplot(3,1,2)
imagesc(ya1,xa1,DEX);
colorbar;
axis equal tight;
subplot(3,1,3)
imagesc(ya1,xa1,DEY);
colorbar;
axis equal tight;


%%%%%%%%%%%%%%%%%%%%%%%%%%%%%%%%%%%%%%%%%%%%%%%%%%%%%%%%%%%%%%%%%%%%%%%%%%%%
%Function called in the previous algorithm to get Bloch wave vector
%%%%%%%%%%%%%%%%%%%%%%%%%%%%%%%%%%%%%%%%%%%%%%%%%%%%%%%%%%%%%%%%%%%%%%%%%%%%

function[Bx,By]=newvector(numvx,numvy)
pointx =[0    0.1047    0.2094    0.3142    0.4189    0.5236    0.6283
0.7330...
    0.8378    0.9425    1.0472    1.1519    1.2566    1.3614    1.4661
1.5708...
    1.6755    1.7802    1.8850    1.9897    2.0944    2.1991    2.3038
2.4086...
    2.5133    2.6180    2.7227    2.8274    2.9322    3.0369    3.1416
3.1416...
    3.1416    3.1416    3.1416    3.1416    3.1416    3.1416    3.1416
3.1416...
    3.1416    3.1416    3.1416    3.1416    3.1416    3.1416    3.1416
3.1416...
    3.1416    3.1416    3.1416    3.1416    3.1416    3.1416    3.1416
3.1416...
    3.1416    3.1416    3.1416    3.1416    3.1416    3.0718    3.0020
2.9322...
    2.8623    2.7925    2.7227    2.6529    2.5831    2.5133    2.4435
2.3736...
    2.3038    2.2340    2.1642    2.0944    2.0246    1.9548    1.8850
1.8151...
    1.7453    1.6755    1.6057    1.5359    1.4661    1.3963    1.3265
1.2566...
    1.1868    1.1170    1.0472    0.9774    0.9076    0.8378    0.7679
0.6981...
    0.6283    0.5585    0.4887    0.4189    0.3491    0.2793    0.2094
0.1396...
    0.0698         0];
```

```
pointy=[ 0         0         0         0         0         0         0
0 ...
         0         0         0         0         0         0         0
0 ...
         0         0         0         0         0         0         0
0 ...
         0         0         0         0         0         0         0
0.1047...
    0.2094    0.3142    0.4189    0.5236    0.6283    0.7330    0.8378
0.9425...
    1.0472    1.1519    1.2566    1.3614    1.4661    1.5708    1.6755
1.7802...
    1.8850    1.9897    2.0944    2.1991    2.3038    2.4086    2.5133
2.6180...
    2.7227    2.8274    2.9322    3.0369    3.1416    3.0718    3.0020
2.9322...
    2.8623    2.7925    2.7227    2.6529    2.5831    2.5133    2.4435
2.3736...
    2.3038    2.2340    2.1642    2.0944    2.0246    1.9548    1.8850
1.8151...
    1.7453    1.6755    1.6057    1.5359    1.4661    1.3963    1.3265
1.2566...
    1.1868    1.1170    1.0472    0.9774    0.9076    0.8378    0.7679
0.6981...
    0.6283    0.5585    0.4887    0.4189    0.3491    0.2793    0.2094
0.1396...
    0.0698         0];
Bx=pointx;
By=pointy;
```

As for the TM-mode FDTD code, the key differences are the update coefficients, which can be analogous to TE-Mode, and the Bloch Periodic Boundary conditions.

Here we just list these important differences

```
%*************************************************************************
*
%     Compute update efficients for Hx, Hy, Dz
%*************************************************************************
*

sigHx=sigx(1:2:Nx2,2:2:Ny2);           % now sigHx and sigHy are
fictitous
sigHy=sigy(1:2:Nx2,2:2:Ny2);           % sigma pointing to  x and y
                                       % directions at the location of
Hx
mHx0=(1/dt)+sigHy/(2*epsz);
mHx1=((1/dt)-sigHy/(2*epsz))./mHx0;
mHx2=-cc./Urxx./mHx0;
mHx3=-(cc*dt/epsz)*sigHx./Urxx./mHx0;
```

```
sigHx=sigx(2:2:Nx2,1:2:Ny2);            % now sigHx and sigHy are
fictitous
sigHy=sigy(2:2:Nx2,1:2:Ny2);            % sigma pointing to  x and y
                                        % directions at the location of
Hy
mHy0=(1/dt)+sigHx/(2*epsz);
mHy1=((1/dt)-sigHx/(2*epsz))./mHy0;
mHy2=-cc./Uryy./mHy0;
mHy3=-(cc*dt/epsz)*sigHy./Uryy./mHy0;

sigDx=sigx(1:2:Nx2,1:2:Ny2);            % now sigDx and sigDy are
fictitous
sigDy=sigy(1:2:Nx2,1:2:Ny2);            % sigma pointing to  x and y
                                        % directions at the location of
Dz
mDz0=(1/dt)+(sigDx+sigDy)/(2*epsz)+sigDx.*sigDy*(dt/4/(epsz^2));
mDz1=(1/dt)-(sigDx+sigDy)/(2*epsz)-sigDx.*sigDy*(dt/4/(epsz^2));
mDz1=mDz1./mDz0;
mDz2=cc./mDz0;
mDz4=-(dt/(epsz^2))*sigDx.*sigDy./mDz0;

%% Drude model parameters
Wp=7.816e15;                            %plasmon frequecy rad/s
wpez=Wp*BEZ;
g=1.673e13;                             %collision frequecy rad/s

%%update efficiency for Ez
mEz0=4*Erzz+2*Erzz*g*dt+(wpez.^2)*(dt^2);
mEz00=mEz0.*BEZ;
mEz1=((2*g*dt+4)./mEz0).*BEZ;
mEz2=((4-2*g*dt)./mEz0).*BEZ;
mEz3=(-8./mEz0).*BEZ;
mEz4=(-(4*Erzz-2*Erzz*g*dt+(wpez.^2)*(dt^2))./mEz0).*BEZ;
mEz5=((8*Erzz-2*(wpez.^2)*(dt^2))./mEz0).*BEZ;


%%%%implementation of periodic boundary conditions in TM mode

     %compute CEx
    for nx=1:Nx
        for ny=1:Ny-1
        CEx(nx,ny)=(Ez(nx,ny+1)-Ez(nx,ny))/dy;
        end
        CEx(nx,Ny)=(phiy*Ez(nx,1)-Ez(nx,Ny))/dy;
    end

%compute CEy

for ny=1:Ny
        for nx=1:Nx-1
        CEy(nx,ny)=-(Ez(nx+1,ny)-Ez(nx,ny))/dx;
        end
```

```
    CEy(Nx,ny)=-(phix*Ez(1,ny)-Ez(Nx,ny))/dx;
end

%Update H Integration

ICEx=ICEx+CEx;
ICEy=ICEy+CEy;

%Update H from curl of E

 Hx=mHx1.*Hx+mHx2.*CEx+mHx3.*ICEx;
 Hy=mHy1.*Hy+mHy2.*CEy+mHy3.*ICEy;



  %compute CHz curl of Hz
    CHz(1,1)=(Hy(1,1)-conj(phix)*Hy(Nx,1))/dx...
             -(Hx(1,1)-conj(phiy)*Hx(1,Ny))/dy;
for nx=2:Nx
    CHz(nx,1)=(Hy(nx,1)-Hy(nx-1,1))/dx...
             -(Hx(nx,1)-conj(phiy)*Hx(nx,Ny))/dy;
end
for ny=2:Ny
    CHz(1,ny)=(Hy(1,ny)-conj(phix)*Hy(Nx,ny))/dx...
              -(Hx(1,ny)-Hx(1,ny-1))/dy;
    for nx=2:Nx
        CHz(nx,ny)=(Hy(nx,ny)-Hy(nx-1,ny))/dx...
                   -(Hx(nx,ny)-Hx(nx,ny-1))/dy;
    end
end

%Update D Integration
        IDz=IDz+Dz;

%Update Dz
        Dz=mDz1.*Dz+mDz2.*CHz+mDz4.*IDz;
```

AS for the FDTD code for 1D periodic structures, just adjust the thickness of PML layer and change the Bloch wave vectors in the code.